Am J Cancer Res 2024;14(8):3711-3732
www.ajcr.us /ISSN:2156-6976/ajcr0149813

Original Article

PCMT1 confirmed as a pan-cancer immune biomarker and a contributor to breast cancer metastasis

Yiqi Liu[1*], Haobing Li[2,3*], Xiangyu Shen[4], Ying Liu[2,3], Xiaoxiao Zhong[4,5], Jing Zhong[2,6], Renxian Cao[2,6]

[1]The First Affiliated Hospital, Hengyang Medical School, University of South China, Hengyang 421001, Hunan, China; [2]Institute of Clinical Medicine, The First Affiliated Hospital, Hengyang Medical School, University of South China, Hengyang 421200, Hunan, China; [3]Department of Medical Oncology, The First Affiliated Hospital, Hengyang Medical School, University of South China, Hengyang 421200, Hunan, China; [4]Department of Breast and Thyroid Surgery, Third Xiangya Hospital, Central South University, Changsha 410000, Hunan, China; [5]Department of General Surgery, Third Xiangya Hospital, Central South University, Changsha 410000, Hunan, China; [6]Institute of Cancer Research, The First Affiliated Hospital, Hengyang Medical School, University of South China, Hengyang 421200, Hunan, China. [*]Equal contributors.

Received February 22, 2023; Accepted August 7, 2024; Epub August 25, 2024; Published August 30, 2024

Abstract: Protein L-isoaspartyl (D-aspartyl) methyltransferase (PIMT, gene name PCMT1) is an enzyme that repairs proteins with altered aspartate residues by methylation, restoring their normal structure and function. This study conducted a comprehensive analysis of PCMT1 in pan-cancer. The Cancer Genome Atlas, Human Protein Atlas website, and the Genotype-Tissue Expression were utilized in analysis of PCMT1 expression. We examined the association between PCMT1 expression and various factors, including gene modifications, DNA methylation, immune cell infiltration, immunological checkpoints, drug susceptibility, tumor mutation burden (TMB), and microsatellite instability (MSI). Enrichment analyses determined the potential biological roles and pathways involving PCMT1. Our focus then shifted to the role of PCMT1 in breast invasive carcinoma (BRCA). We found that PCMT1 expression was aberrant in many tumors and significantly influenced the prognosis across several cancer types. Gene alterations in PCMT1 predominantly involved deep deletions and amplifications. A negative correlation was observed between DNA methylation and PCMT1 expression across all studied cancer types except thyroid carcinoma PCMT1 exhibited positive correlations with common lymphoid progenitor and CD4(+) T helper 2 cells, whereas it was inversely correlated with central and effector memory T cells, memory CD8(+) T cells, and CD4(+) T helper 1 cells. In many cancer types, PCMT1 expression closely correlated with immunological checkpoint inhibitors, TMB, and MSI. It was also significantly linked to pathways involved in epithelial-mesenchymal transition (EMT), highlighting its role in cancer metastasis. PCMT1 emerged as a significant predictor of breast cancer progression. In vitro experiments demonstrated that reducing PCMT1 expression decreased BRCA cell migration and invasiveness. Additionally, animal studies confirmed that inhibition of PCMT1 slowed tumor growth.

Keywords: PCMT1, pan-cancer, immune infiltration, prognosis biomarker, breast invasive carcinoma

Introduction

Globally, cancer remains a significant health concern and is a leading cause of mortality [1]. According to recent statistics, lung cancer is the most lethal, accounting for 18% of cancer-related deaths, followed by colorectal cancer (9.4%), liver cancer (8.3%), stomach cancer (7.7%), and breast cancer (BC) in women (6.9%) [2]. Despite advances in cancer research that have improved prevention and treatment methodologies, the overall cure rate for cancer patients remains low worldwide [3]. Immunotherapy has become a focal point in oncology, significantly improving patient prognosis. However, it faces several challenges, including unpredictable efficacy, limited response rates, and potential autoimmune reactions [4]. Therefore, there is a pressing need to identify more specific and sensitive biomarkers to elucidate the relationship between cancer and immunity and to understand the molecular processes underlying cancer progression for early detection and treatment. The advancement of

https://doi.org/10.62347/TYLL7952

bioinformatics and the availability of public cancer databases have facilitated pan-cancer studies, allowing for a more comprehensive and in-depth investigation of tumor progression mechanisms.

Under specific conditions, residues of L-aspartic acid (L-Asp) and L-asparagine (L-Asn) can transform into L-isoaspartic acid (L-isoAsp), D-isoaspartic acid (D-isoAsp), and D-aspartic acid (D-Asp), resulting in structurally dysfunctional proteins [5]. These abnormal aspartic acid residues are addressed through specific repair pathways. An enzyme, protein L-isoaspartyl (D-aspartyl) methyltransferase (PIMT, gene name PCMT1), plays a crucial role by recognizing and methylating proteins containing these modified aspartate residues, which are then spontaneously reverted to normal aspartate, thus restoring the protein's normal structure and function [6]. PCMT1 is widely distributed across mammalian tissues, with high concentrations in the central nervous system (CNS), implicating its role in various neurological disorders such as Alzheimer's disease, Parkinson's disease, and multiple sclerosis [7-11]. The human PCMT1 gene is polymorphic, with at least four known variants [12]. Research suggests that polymorphisms in the PCMT1 gene may contribute to premature ovarian failure by impacting the reproductive cycle [13]. Additionally, PCMT1 influences metabolic processes, including cardiac energy metabolism through interactions with nuclear receptor coactivators [14], amino acid metabolism [15], and regulation of hepatic gluconeogenesis [16].

Recent investigations have highlighted PCMT1's critical role in cancer, associating it with poorer prognosis in several malignancies including bladder cancer [17], lung adenocarcinoma (LUAD) [18], BC [19], and ovarian cancer (OC) [20]. PCMT1 is known to inhibit apoptosis in SH-SY5Y neuroblastoma cells, potentially through cellular antioxidant mechanisms [21]. Furthermore, PCMT1 plays a crucial role in angiogenesis by mediating the effects of vascular endothelial growth factor [22]. Studies have shown that PCMT1 is instrumental in tumor metastasis and invasion. Specifically, PCMT1 expression is an independent negative prognostic factor in bladder cancer and is significantly associated with clinical stage, metastasis, and tumor infiltration [17]. In bladder cancer, PCMT1 influences migration and invasiveness by regulating the expression of genes related to epithelial-mesenchymal transition (EMT) [17]. A recent study on OC suggests that PCMT1 drives metastasis and resistance to apoptosis, with the PCMT1-ECM protein LAMB3 combination activating the integrin-FAK-Src pathway, thereby enhancing cancer cell adhesion, migration, and invasion [20]. However, research on PCMT1 in the context of tumors is still limited, and its role across multiple cancer types has not been thoroughly explored.

Using data from the Cancer Genome Atlas (TCGA) and the Genotype-Tissue Expression (GTEx) projects, this study provides a comprehensive analysis of PCMT1 across various cancers. It examines its expression levels, clinical characteristics, prognostic value, and involvement in biological processes and pathways. We also explore the association between PCMT1 expression and tumor immunity, immunological checkpoints, DNA methylation, genetic alterations, tumor mutational burden (TMB), and microsatellite instability (MSI) in a pan-cancer context. Additionally, a series of in vitro experiments were conducted to investigate PCMT1's biological functions in breast invasive carcinoma (BRCA) cells, focusing on tumor cell migration, invasion, and proliferation.

Materials and methods

PCMT1 expression and data collection

To analyze PCMT1 expression across various cancers, we sourced RNAseq clinical data from the TCGA (https://www.portal.gdc.cancer) and GTEx (https://www.genome.gov/) database, comprising 10,960 cancer samples from TCGA and 15,841 normal samples from GTEx. Statistical analyses were conducted using the "limma" and "ggpubr" packages in R software v4.0.3, with p-values <0.05 deemed statistically significant. Additionally, we explored the specificity of PCMT1 mRNA expression across different tissues, single cell types, and tissue-specific cell types using data from the Human Protein Atlas (HPA, https://www.proteinatlas.org/).

PCMT1 prognostic analysis

PCMT1 RNAseq expression profiles and associated clinical data for 33 cancer types were

obtained from TCGA. We utilized Kaplan-Meier (K-M) and univariate Cox regression analyses to investigate the association between PCMT1 expression and overall survival (OS), disease-free survival (DFS), and progression-free survival (PFS) across cancers, using the R packages "survival" and "survminer".

Immunological analysis of PCMT1 in pan-cancer

Given the strong correlation between immunological cell infiltration and cancer progression [23], we conducted a correlation analysis between PCMT1 expression and levels of immunological cell infiltrates using the "immunedeconv" R package [24]. Correlation coefficients were calculated using the Spearman method. Immunological checkpoint inhibitor therapies (ICIs) have significantly extended patient survival across various tumor types [25]. TMB and MSI are known predictors of response to ICIs; TMB as an indicator of tumor mutational load [26] and MSI resulting from mismatch repair system defects [27]. In our study, we assessed the correlation between PCMT1 expression and eight immunological checkpoints: CD274, SIGLEC15, CTLA-4, HAVCR2, PDCD1, LAG3, PDCD1LG2, and TIGIT. Further correlation analyses between PCMT1 and TMB and MSI were performed across pan-cancer, to elucidate the potential role of PCMT1 in tumor immunology.

Functional enrichment analysis of PCMT1-related genes

We utilized the STRING database (https://string-db.org/) to explore the co-expression network of PCMT1 in Homo sapiens. The network was configured as follows: network type set to full STRING, edge meaning based on evidence, active interaction sources limited to co-expression, minimum interaction score set at low confidence (0.150), and a maximum of 50 interactors included. Additionally, the "Similar Gene Detection" module of GEPIA2 (http://gepia2.cancer-pku.cn/) was used to extract the hundred genes most similarly expressed to PCMT1 from a dataset containing 9,736 tumor samples and 8,587 normal samples from TCGA and GTEx, respectively. Data from STRING and GEPIA2 were combined to perform Gene Ontology (GO) and Kyoto Encyclopedia of Genes and Genomes (KEGG) analyses using the "clusterProfiler" R package [30]. Further, the "Network" module of the Biological General Repository of Interaction Datasets (BioGRID) (https://thebiogrid.org/) helped generate a PCMT1-protein interaction network with a "concentric circles" topology.

Gene set cancer analysis (GSCA)

GSCA is a comprehensive platform integrating genomic, immunogenomic, and pharmacogenomic cancer analyses. We accessed data on DNA methylation levels of PCMT1 provided by GSCA (http://bioinfo.life.hust.edu.cn/GSCA/#/). The association between PCMT1 DNA methylation and expression in human cancers was examined, along with the relationship between PCMT1 DNA methylation levels and cancer prognostic values. We also investigated the interaction between PCMT1 and prominent cancer-related pathways, including RTK, RAS/MAPK, DNA Damage Response, Apoptosis, ER Hormone, AR Hormone, TSC/mTOR, EMT, Cell Cycle, and PI3K/AKT.

Genetic alteration analysis

We employed cBioPortal (https://www.cbioportal.org/) to obtain genetic alteration data for PCMT1. Using the "Cancer Type Summary" module, we calculated the gene mutation frequency and PCMT1 copy number changes across all TCGA cancer types. Additionally, the "Mutation" module was utilized to generate a mutation site plot for PCMT1.

Correlation analysis of PCMT1 expression with clinical factors and immune infiltration in BRCA

We acquired RNAseq and clinical data from TCGA for BRCA projects. Univariate and multivariate Cox regression analyses were used to determine if PCMT1 serves as an independent predictive factor in BRCA. The diagnostic value of PCMT1 in BRCA was evaluated using the receiver operating characteristic curve (ROC), generated with the "pROC" and "ggplot2" packages in R. Additionally, we developed a nomogram incorporating PCMT1 expression and clinicopathological features. Immune infiltration analysis was performed using the single sample GSEA (ssGSEA) method through the GSVA package, and the classification of the 24 immune cell types referenced is detailed in

[31]. Correlations between PCMT1 and levels of immunological cell infiltration were assessed using Spearman's technique and the Wilcoxon rank-sum test, with a *p*-value <0.05 indicating statistical significance.

Cell culture

Cell lines used in this study, including MCF-7, MDA-MB-231, MDA-MB-453, HCC1806, and T47D cells, were provided by Prof. Xuyu Zu of The First Affiliated Hospital of University of South China. MDA-MB-231, T47D, and MDA-MB-453 cells were cultured in high-glucose DMEM (Gibco), while HCC1806 cells were maintained in RPMI 1640 medium (Gibco), and MCF-7 cells in MEM medium (Procell). All media were supplemented with 10% fetal bovine serum (FBS; Gibco) and cells were incubated in a 5% CO_2 environment at 37°C.

Establishment of knockdown cell lines

To silence PCMT1 expression in BRCA cell lines, lentiviral vectors carrying shRNAs targeting PCMT1 (sh-PCMT1#1, sh-PCMT1#2, and sh-PCMT1#3) and a control shRNA (sh-NC) were used, produced by Shanghai GeneChem (Shanghai, China). Cells were infected with lentivirus for 48 hours, followed by selection with puromycin to establish stable cell lines. Spread a certain number of cells evenly on a 6-well plate, add a certain concentration gradient of puromycin (0-15 μg/ml) to 3 mL of culture medium, and incubate for 48 hours. The selective culture medium should be changed every 2 days. Evaluate cell survival rate using trypan blue and stain every 2 days. After 3 to 5 days of antibiotic selection, it was found that 2 μg/ml of puromycin was the minimum screening concentration for killing all cells, so this concentration was used for the selection plan.The sequences of these shRNAs are provided in Supplementary Table 1.

Quantitative real-time PCR

RNAiso Plus reagent (9108, Japan) was utilized to extract RNA from BRCA cells. RNA was then reverse transcribed into cDNA through PrimeScript™ RT Master Mix (RR036A, TaKaRa, Japan). qPCR was conducted on a real-time PCR detection system with TB Green®Premix Ex Taq™ II (RR820A, TaKaRa, Japan). Reaction occurred at 37.0°C for 15 minutes, followed by 85.0°C for 5 s, and 4°C for 15 s. Expression levels were standardized to endogenous control β-actin. We calculated the relative expression of PCMT1 mRNA in BRCA cells using the $2^{-\Delta\Delta Ct}$ method. mRNA expression was analyzed via GraphPad Prism 8 software. The sequences of the primers were listed in Supplementary Table 1.

Western blot analysis

Total protein from BRCA cells was isolated using radio immunoprecipitation assay (RIPA) lysis buffer (01408/35020, CWBIO, Beijing, China), according to the manufacturer's instructions. Protein lysates (50 μg) were separated on 12% SDS-PAGE gels for Western blot analysis and transferred onto 0.45 μm polyvinylidene difluoride (PVDF) membranes. Membranes were incubated overnight with primary antibodies against β-actin (1:1000, 20536-1-AP) and PCMT1 (1:1000, 10519-1-AP), followed by HRP-conjugated secondary antibodies (1:3000, SA00001-2, Proteintech, USA). Detection was performed using ECL ultra (P10100, NCM biotech, Suzhou, China).

Cell proliferation assay

MDA-MB-231 and HCC1806 cells infected with shRNA-PCMT1 lentivirus were trypsinized at 90% confluency and seeded into a 96-well plate at 3×10^3 cells per well, with six replicates per group. The experiment included three groups: siPCMT1, empty vector, and treatment-free. Cell viability was assessed at 0, 24, 48, 72, and 96 hours using the Cell Counting Kit-8 (CCK-8, AWC0114a, Abiowell, China).

Transwell migration and invasion assay

Migration assays were conducted using Transwell chambers without Matrigel, while invasion assays utilized chambers coated with Matrigel (Corning, USA). For invasion assays, 30 μl of Matrigel was added to the upper chamber one day prior. Cells (5×10^4) in 300 μl of serum-free medium were placed in the upper chamber, and 500 μl of medium containing 10% FBS was added to the lower chamber. After 48 hours at 37°C, cells on the lower surface were fixed with 4% formaldehyde for 15 minutes and stained with 0.1% crystal violet in ammonium oxalate solution (Solarbio, Beijing, China) for 10 minutes. Cells were then counted and imaged under an inverted microscope.

Construction of subcutaneous tumors and metastases in nude mice

All animal experiments were conducted in compliance with the "Guidelines for the Care and Use of Laboratory Animals" and approved by the Hospital's Board of Directors. Female BALB/c nude mice (Slack and Jingda), aged 4-6 weeks, were injected subcutaneously and via the caudal vein with 1×10^7/200 μL of BC cells (MDA-MB-231, HCC1806). Tumor growth was monitored every two days, and tumor size and weight were recorded. After three weeks, the mice were euthanized, and tissues including tumors, liver, lung, kidney, and brain were analyzed by HE staining.

Statistical analysis

Experimental data were analyzed by t-test, and one-way ANOVA using GraphPad Prism 9 (Dotmatics, Boston, MA, USA) software. Forest plots, illustrating *P* values, hazard ratios (HRs), and 95% confidence intervals (CIs), were generated with the "forestplot" package in R. A *p*-value <0.05 indicated statistical significance.

Results

Expression levels of PCMT1 in human pan-cancer and corresponding normal tissues

From TCGA, we initially examined differences in PCMT1 mRNA expression between tumor and non-tumor tissues across 33 different cancers. Violin plots (**Figure 1A**) revealed that PCMT1 levels were significantly elevated in several cancers including BRCA, cervical squamous cell carcinoma and endocervical adenocarcinoma (CESC), cholangiocarcinoma (CHOL), colon adenocarcinoma (COAD), diffuse large B-cell lymphoma (DLBC), esophageal carcinoma, head and neck squamous cell carcinoma (HNSCC), liver hepatocellular carcinoma (LIHC), lung squamous cell carcinoma, pancreatic adenocarcinoma (PAAD), pheochromocytoma and paraganglioma (PCPG), prostate adenocarcinoma (PRAD), rectum adenocarcinoma (READ), skin cutaneous melanoma (SKCM), stomach adenocarcinoma (STAD), thyroid carcinoma (THCA), thymoma (THYM), and uterine carcinosarcoma (UCS). Conversely, significant downregulation of PCMT1 was observed in glioblastoma multiforme, kidney chromophobe (KICH), kidney renal clear cell carcinoma (KIRC), kidney renal papillary cell carcinoma (KIRP), acute myeloid leukemia (LAML), lower grade glioma (LGG), LUAD, and testicular germ cell tumors (TGCT).

In addition, we analyzed the protein expression of PCMT1 between tumor and non-tumor tissues in 10 different cancers. Results (**Figure 1B**) illustrated that, PCMT1 levels were significantly higher in nine malignancies, including BC, colon cancer, OC, uterine corpus endometrial carcinoma (UCEC), lung cancer, PAAD, HNSCC, glioblastoma, and liver cancer. However, a significant decrease in PCMT1 expression was detected in clear cell renal cell carcinoma.

The HPA website was used to explore PCMT1 mRNA expression levels in various human tissues and cell lines. Analysis using a consensus dataset, which combines HPA transcriptomics and GTEx transcriptomics datasets, revealed that PCMT1 is broadly expressed across numerous tissues, although its expression specificity is low (Supplementary Figure 1A). PCMT1 was found to be highly expressed in different single cell types, with the highest levels observed in early spermatids (Supplementary Figure 1B). Moreover, PCMT1 is mainly enriched in cardiomyocytes, early spermatids, and thyroid glandular cells across various tissue-specific cell types (Supplementary Figure 1C).

Prognostic value of PCMT1 in pan-cancer

To evaluate the prognostic value of PCMT1 in pan-cancer settings, K-M survival and univariate Cox regression analyses were conducted. K-M curves indicated that elevated PCMT1 expression was associated with poorer OS in bladder cancer (BLCA), HNSCC, LIHC, BRCA, LUAD, and mesothelioma (MESO) (**Figure 2A-F**). Conversely, reduced PCMT1 levels correlated with better OS in KIRC and READ (**Figure 2G**, **2H**). Univariate Cox regression analysis further confirmed that PCMT1 overexpression served as a risk factor in BLCA, BRCA, LIHC, LUAD, MESO, and HNSCC, but acted as a protective factor in cancers such as KIRC and READ (**Figure 3A**). Forest plots from the Cox regression analysis (**Figure 3B**) revealed that PCMT1 expression significantly impacted DFS in KIRP, LGG, and THCA. For PFS, univariate analysis (**Figure 3C**) suggested that PCMT1 played a protective role in KIRC, LGG, and THCA, while high PCMT1 expression was linked

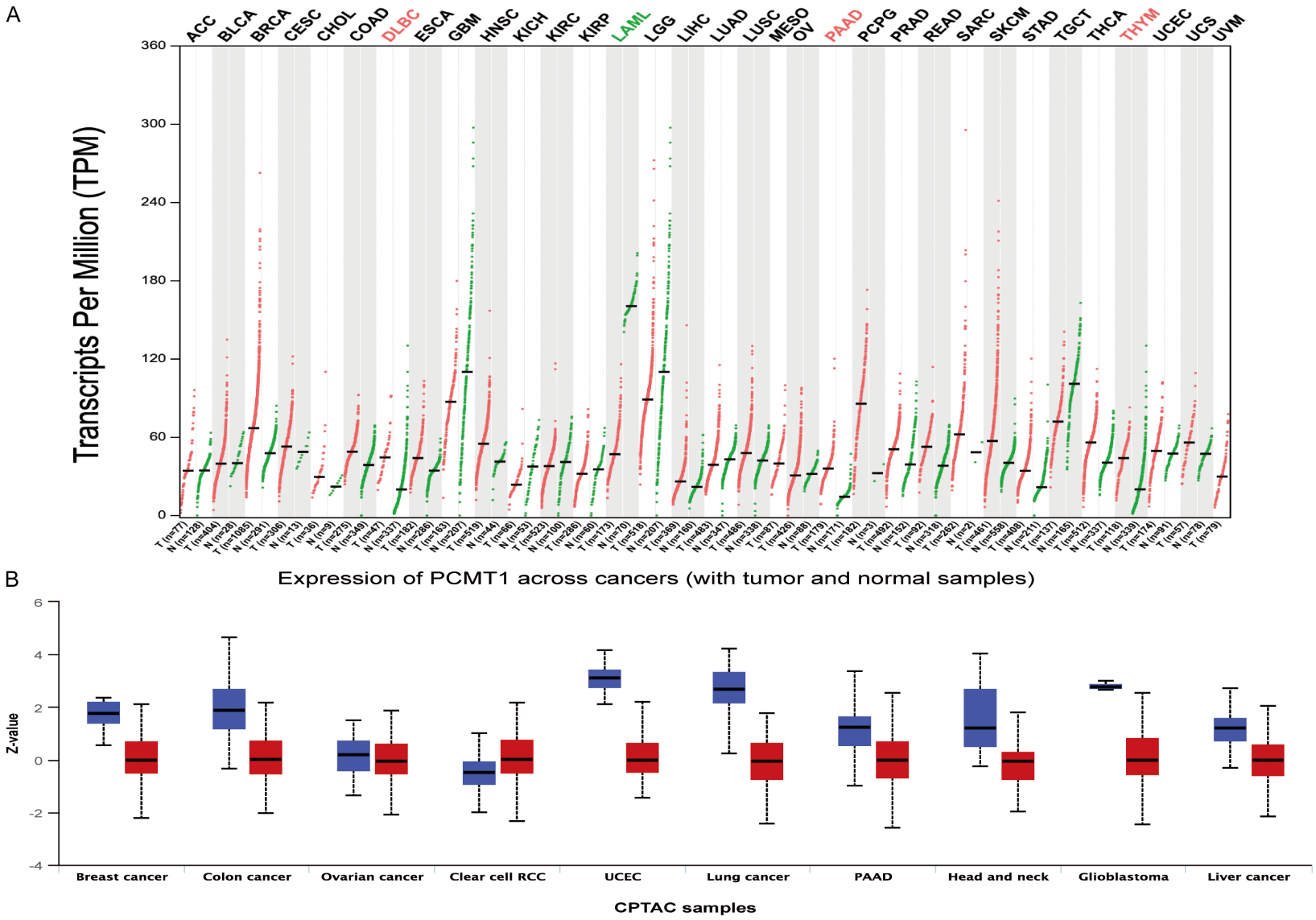

Figure 1. PCMT1 was differentially expressed in tumor and normal tissues. A. The mRNA expression of PCMT1 in pan-cancerous tissues of the TCGA database. red meas tumor and green means normal (http://gepia2.cancer-pku.cn/). B. The protein expression of PCMT1 in pan-cancerous tissues of CPTAC samples, red meas tumor and blue means normal (https://ualcan.path.uab.edu). *P<0.05; **P<0.01; and ***P<0.001.

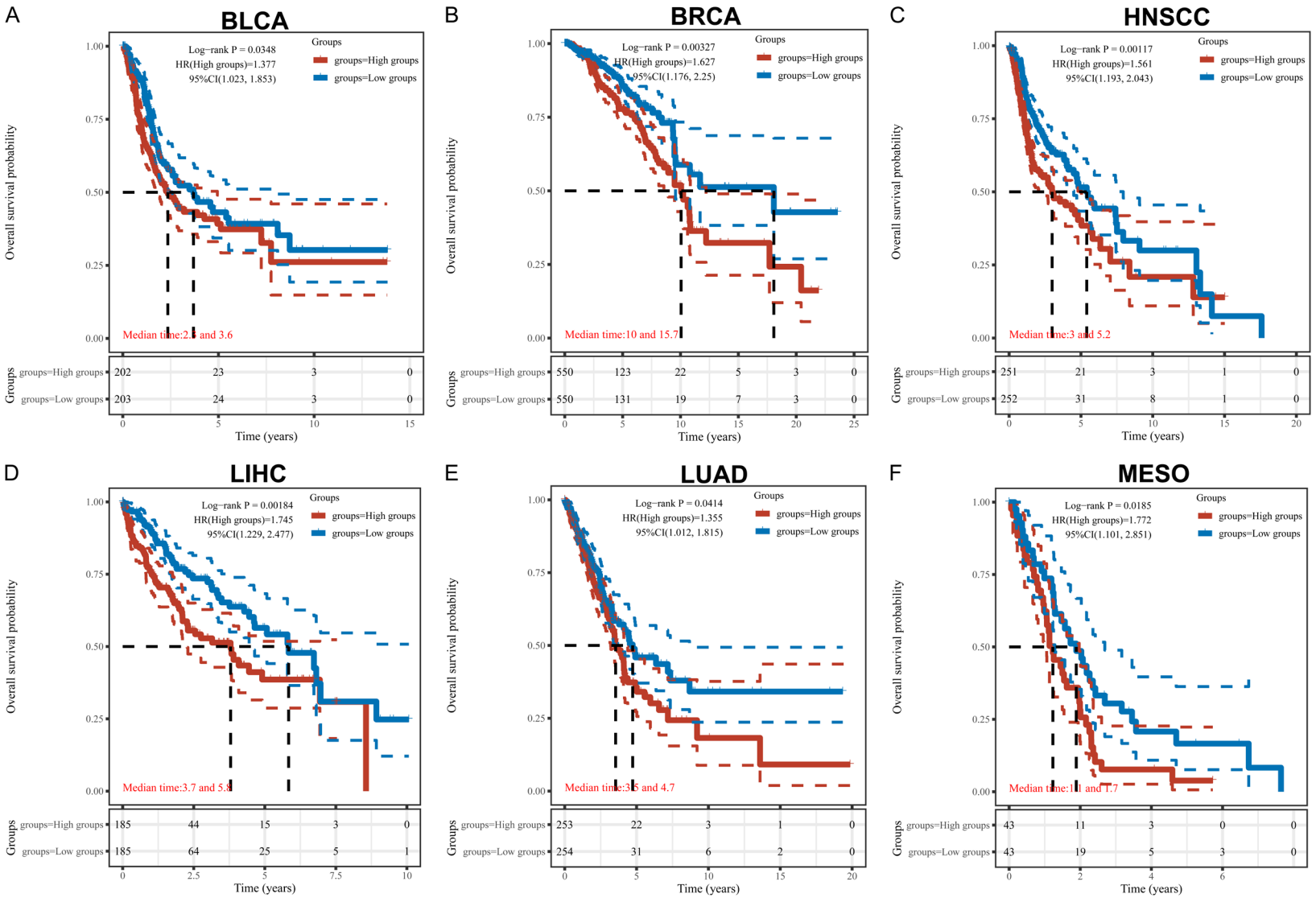
A
BLCA
Log−rank P = 0.0348
HR(High groups)=1.377
95%CI(1.023, 1.853)
Groups
groups=High groups
groups=Low groups
Median time:2.6 and 3.6
Overall survival probability
Groups
groups=High groups 202 23 3 0
groups=Low groups 203 24 3 0
Time (years)
B
BRCA
Log−rank P = 0.00327
HR(High groups)=1.627
95%CI(1.176, 2.25)
Groups
groups=High groups
groups=Low groups
Median time:10 and 15.7
Overall survival probability
Groups
groups=High groups 550 123 22 5 3 0
groups=Low groups 550 131 19 7 3 0
Time (years)
C
HNSCC
Log−rank P = 0.00117
HR(High groups)=1.561
95%CI(1.193, 2.043)
Groups
groups=High groups
groups=Low groups
Median time:3 and 5.2
Overall survival probability
Groups
groups=High groups 251 21 3 1 0
groups=Low groups 252 31 8 1 0
Time (years)
D
LIHC
Log−rank P = 0.00184
HR(High groups)=1.745
95%CI(1.229, 2.477)
Groups
groups=High groups
groups=Low groups
Median time:3.7 and 5.8
Overall survival probability
Groups
groups=High groups 185 44 15 3 0
groups=Low groups 185 64 25 5 1
Time (years)
E
LUAD
Log−rank P = 0.0414
HR(High groups)=1.355
95%CI(1.012, 1.815)
Groups
groups=High groups
groups=Low groups
Median time:3.5 and 4.7
Overall survival probability
Groups
groups=High groups 253 22 3 1 0
groups=Low groups 254 31 6 2 0
Time (years)
F
MESO
Log−rank P = 0.0185
HR(High groups)=1.772
95%CI(1.101, 2.851)
Groups
groups=High groups
groups=Low groups
Median time:1.1 and 1.7
Overall survival probability
Groups
groups=High groups 43 11 3 0 0
groups=Low groups 43 19 5 3 0
Time (years)

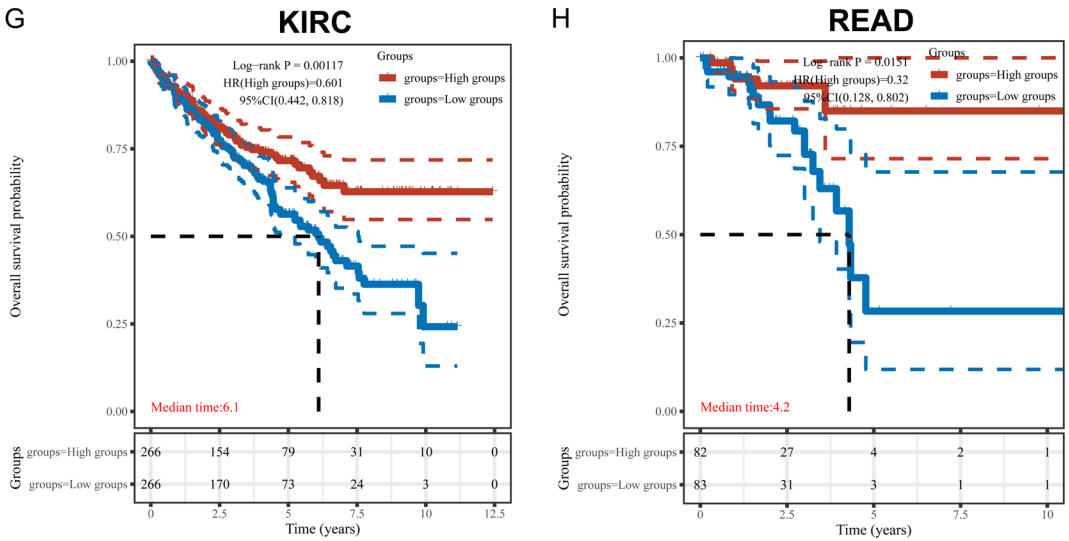

Figure 2. The relationship between PCMT1 expression profile and overall survival (OS) of patients with different tumors was analyzed by Kaplan-Meier survival method. (A) BLCA, (B) BRCA, (C) HNSCC, (D) LIHC, (E) LUAD, (F) MESO, (G) KIRC, (H) READ. BLCA: bladder cancer, BRCA: breast invasive carcinoma, HNSCC: head and neck squamous cell carcinoma, LIHC: liver hepatocellular carcinoma, LUAD: lung adenocarcinoma, MESO: mesothelioma, KIRC: kidney renal clear cell carcinoma, READ: rectum adenocarcinoma.

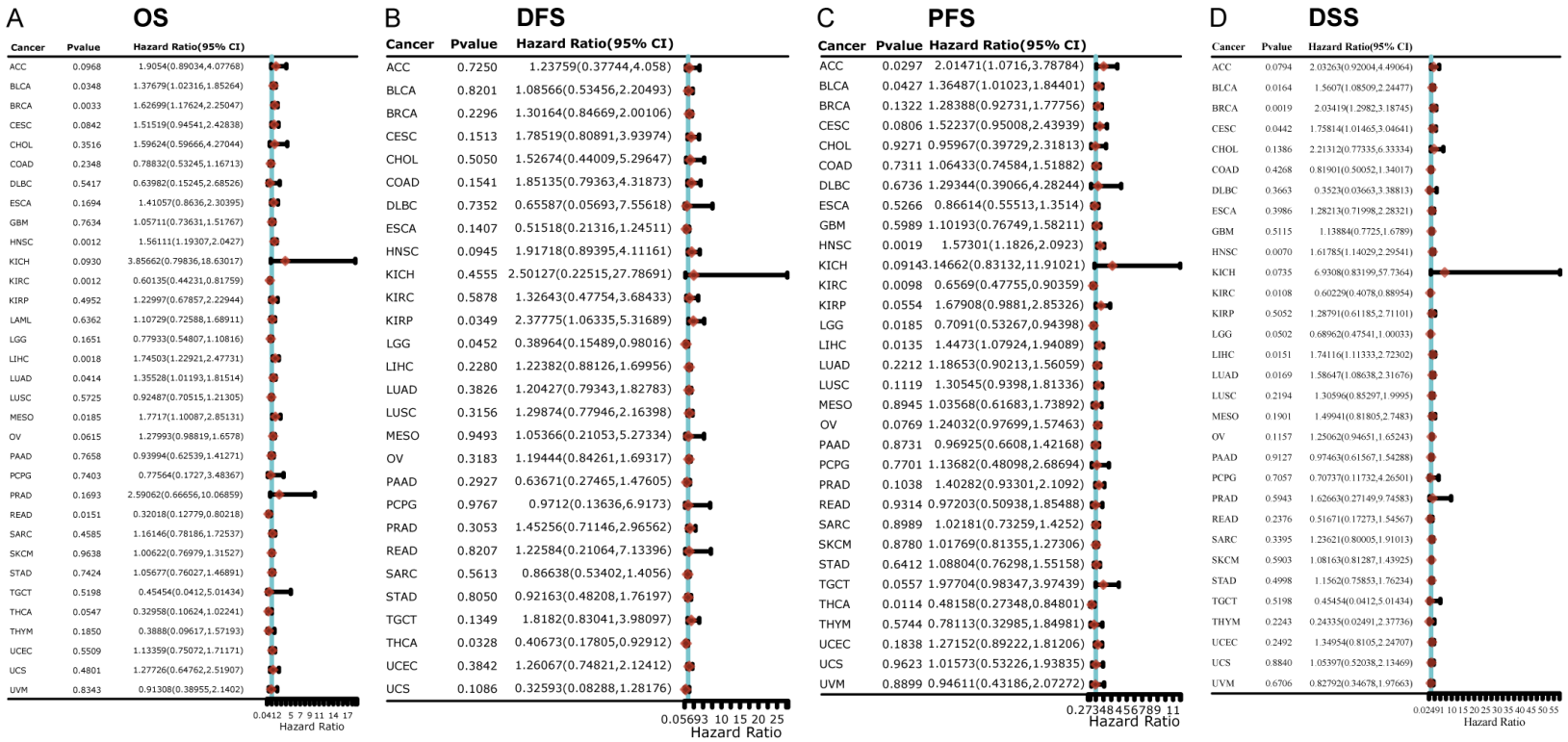

Figure 3. Association of PCMT1 expression and pan-cancer overall survival (OS), disease-free survival (DFS), progression-free survival (PFS), and disease-specific survival (DSS) based on univariate Cox regression analysis. A. Correlation between PCMT1 expression and OS. B. Correlation between PCMT1 expression and DFS. C. Correlation between PCMT1 expression and PFS. D. Correlation between PCMT1 expression and DSS.

with worse PFS in ACC, BLCA, HNSC, and LIHC. Disease-specific survival (DSS) analysis indicated that elevated PCMT1 expression was a risk factor in BLCA, BRCA, CESC, HNSC, LIHC, and LUAD (**Figure 3D**).

Genetic alterations and methylation landscapes of PCMT1 in different tumors

Data on PCMT1 genetic alterations were sourced from cBioPortal. The analysis showed that deep deletion and amplification were the primary modes of gene alteration across all TCGA tumor types, with high-frequency alterations observed in UVM (7.50%, predominantly deep deletions), DLBC (6.25%, predominantly deep deletions), and SARC (Sarcoma) (5.88%, predominantly amplifications) (Supplementary Figure 2A). Missense mutations were the most common mutation type (Supplementary Figure 2B). Additionally, the GCSA database provided insights into the DNA methylation of PCMT1 across different tumors. A plot of associations between DNA methylation levels and PCMT1 expression in pan-cancer demonstrated generally negative correlations, except in THCA (Supplementary Figure 2C). Elevated DNA methylation of PCMT1 was associated with better PFS in UCEC and BLCA, and worse PFS in HNSC, THCA, KIRC, and DLBC (Supplementary Figure 3A-F). For OS, increased DNA methylation levels of PCMT1 were linked to worse outcomes in HNSC, KIRC, and DLBC (Supplementary Figure 3G-I). For DSS, higher DNA methylation levels of PCMT1 correlated with worse DSS in HNSC and KIRC (Supplementary Figure 3J, 3K). Finally, for disease-free interval (DFI), elevated DNA methylation of PCMT1 was associated with worse DFI in KIRC and better DFI in UCEC (Supplementary Figure 3L, 3M).

Correlation analysis of PCMT1 expression with tumor microenvironment and immune cell infiltration in pan-cancer

The heatmap analysis indicated a significant positive correlation between PCMT1 expression and CD8+ T cell infiltration in 14 different malignancies (Supplementary Figure 4A). In KIRC and LIHC, PCMT1 expression was positively associated with the infiltration levels of all six immunological cell types analyzed (Supplementary Figure 4A). Further analysis using the xCell algorithm revealed significant associations between PCMT1 expression and stromal scores, the microenvironment, and immune scores in most tumors (Supplementary Figure 4B). PCMT1 expression was also positively correlated with CD4+ T helper 2 (Th2) cells and negatively correlated with central and effector memory T cells, CD8+ memory T cells, and CD4+ T helper 1 (Th1) cells in the majority of tumors (Supplementary Figure 4B). Notably, BRCA, KIRC, SKCM, TGCT, THCA, and THYM showed significant links to the majority of immunological infiltrate cells (Supplementary Figure 4B). These findings suggest that PCMT1 expression is strongly related to immune infiltrations across cancers.

Correlation analysis of PCMT1 and immune checkpoints

Heatmap results (**Figure 4A**) demonstrated correlations between PCMT1 expression and eight immunological checkpoints across multiple tumors, highlighting potential targets for immunotherapy. CD274 expression positively correlated with PCMT1 in multiple cancers, including KIRP, BLCA, KIRC, LIHC, PAAD, LUAD, OV, PCPG, SKCM, PRAD, STAD, UCEC, KICH, and UVM (all p-values <0.05). Similarly, PCMT1 expression was positively associated with CTLA4 in BLCA, KIRP, LIHC, LUAD, OV, PAAD, and UVM (all p-values <0.05). HAVCR2 expression was positively correlated with PCMT1 in ACC, BLCA, COAD, KIRC, LAML, LIHC, LUAD, OV, PAAD, PRAD, UCEC, and UVM (all p-values <0.05). LAG3 expression was positively linked with PCMT1 in seven cancers: BLCA, OV, LIHC, LUAD, UCEC, PAAD, and UVM (all p-values <0.05). PDCD1 expression correlated positively with PCMT1 in UVM, LIHC, OV, LUAD, PAAD, THYM, and KIRP (all p-values <0.05). PDCD1LG2 expression also showed a positive relationship with PCMT1 in a broad range of tumors including BLCA, KIRC, COAD, HNSC, KICH, LIHC, KIRP, LUAD, OV, PAAD, PCPG, SKCM, UCEC, PRAD, and UVM (all p-values <0.05). A positive association was found between SIGLEC15 and PCMT1 in KICH, LAML, KIRC, OV, KIRP, PCPG, THCA, PRAD, and THYM (all p-values <0.05). Lastly, TIGIT expression positively correlated with PCMT1 in BLCA, KIRP, OV, LIHC, PAAD, LUAD, UCEC, and UVM (all p-values <0.05), further underlining the diverse immunological roles of PCMT1 across cancer types.

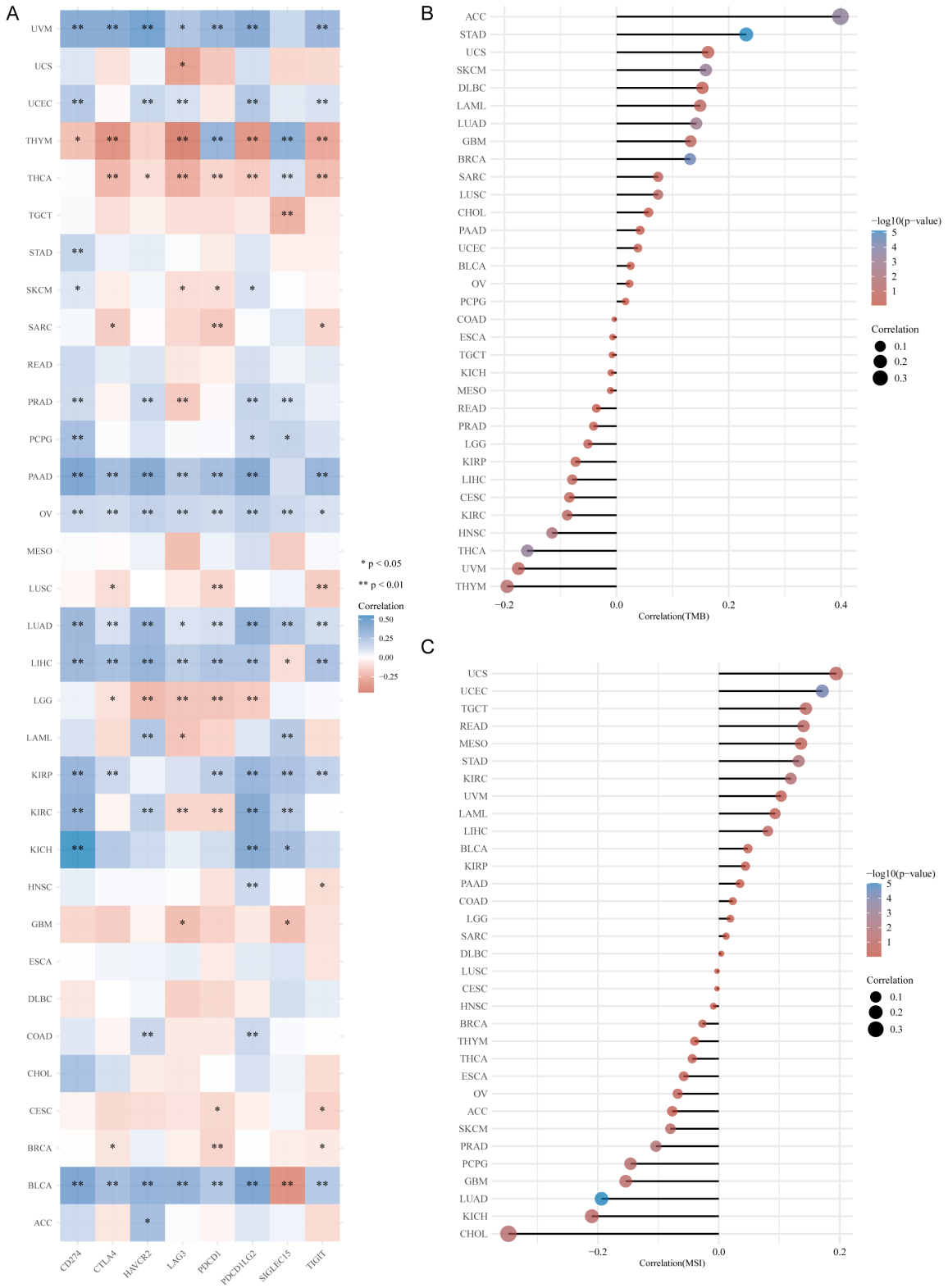

Figure 4. Association between PCMT1 expression and various tumor immune checkpoint inhibitor therapies (ICIs). A. Relationship between PCMT1 expression and 8 immune checkpoint-related genes. B. Relationship between PCMT1 expression and tumor mutational burden (TMB). C. Correlation between PCMT1 expression and microsatellite instability (MSI). *P<0.05; **P<0.01.

Correlation between PCMT1 expression and TMB and MSI

TMB is an indicator of the mutation rate within a tumor, and MSI reflects a hypermutation pattern due to defects in the mismatch repair system [26, 27]. Both TMB and MSI are considered prognostic biomarkers for responsiveness to immune checkpoint inhibitors (ICIs) [28, 29]. Our analysis investigated the relationship between PCMT1 expression across various cancers with TMB and MSI. Results showed a strong positive correlation between PCMT1 expression and TMB in ACC, BRCA, LUAD, SKCM, and STAD, with the strongest association observed in ACC (Spearman's R=0.399, P=3.36E-04) (**Figure 4B**). In contrast, PCMT1 expression was negatively correlated with TMB in HNSC, THCA, and THYM. Regarding MSI, PCMT1 expression was positively correlated with MSI in KIRC, STAD, and UCEC, but negatively associated in CHOL, LUAD, PCPG, and PRAD (**Figure 4C**). These findings underscore the complex interplay between PCMT1 expression and genetic instability markers, potentially influencing the effectiveness of immunotherapy strategies.

Correlation analysis of PCMT1 and drug susceptibility

Analysis from the Genomics of Drug Sensitivity in Cancer (https://www.cancerrxgene.org/) database revealed that PCMT1 potentially influences the response to most drugs (all *p*-values <0.05); however, it was not significantly associated with FK866, CP466722, TG101348, or TPCA-1 (**Figure 5A**). Conversely, data from the Cancer Therapeutics Response Portal (CTRP) indicated that PCMT1 had no significant impact on most drugs, with a notable exception being a potential effect on LY2183240 (all *p*-values <0.05) (**Figure 5B**). These findings suggest that PCMT1 might modulate drug sensitivity and tolerance in various cancers, though its role appears to vary depending on the specific agent.

Functional enrichment analysis of PCMT1-related genes

To elucidate the molecular mechanisms of PCMT1 in tumorigenesis, a series of analyses were conducted. Initially, a co-expression network was constructed using the STRING database to identify 50 proteins interacting with PCMT1 (**Figure 6A**). Subsequently, the 100 genes most similarly expressed to PCMT1 were extracted from GEPIA2. These 150 gene combinations from STRING and GEPIA2 underwent further enrichment analysis for GO and KEGG. As depicted in **Figure 6B**, the top GO biological process terms included antigen processing and presentation. The cellular components were primarily the proteasome complex, endopeptidase complex, and peptidase complex, while the molecular functions focused on ubiquitin conjugating enzyme activity, ubiquitin-like protein conjugating enzyme, and threonine-type endopeptidase activity. The top KEGG pathways identified were Alzheimer's disease, Parkinson's disease, and pathways of neurodegeneration-multiple diseases (**Figure 6B**). Furthermore, the PCMT1-protein interaction network from the BioGRID 4.4 database highlighted significant interactions with TP53, CUL3, BRCA1, LMNA, MYC, and UBC (**Figure 6C**). Analysis using the GCSA website revealed PCMT1's close links to apoptosis, cell cycle, and EMTpathways (**Figure 6D**).

Clinical relevance and immune infiltration analyses of PCMT1 in BRCA

PCMT1 expression was notably elevated in BRCA and strongly associated with OS (**Figure 3A**) and DSS (**Figure 3D**) in BRCA patients, indicating a potential critical role in BRCA development and progression. Univariate and multivariate analyses identified high PCMT1 expression as an independent risk factor for poor BRCA prognosis. Factors such as T stage, N stage, pathological stage, menopause status, age, and radiation therapy also influenced OS (all P<0.05) (Supplementary Table 2). Additionally, a receiver operating characteristic (ROC) curve yielded an area under the curve (AUC) of 0.779, demonstrating the robust diagnostic value of PCMT1 in BRCA (**Figure 7A**). A nomogram and prediction model developed using Cox regression analysis for internal validation showed a c-index of 0.816 (95% CI: 0.782-0.849) (**Figure 7B**). Furthermore, PCMT1 expression inversely correlated with plasmacytoid dendritic cell (pDC) infiltration and positively with Th2 cells (P<0.001, **Figure 7C**, **7D**). The correlation coefficients were -0.35 (**Figure 7E**) for PCMT1 and pDC, and 0.34 (**Figure 7F**) for PCMT1 and Th2 cells (R).

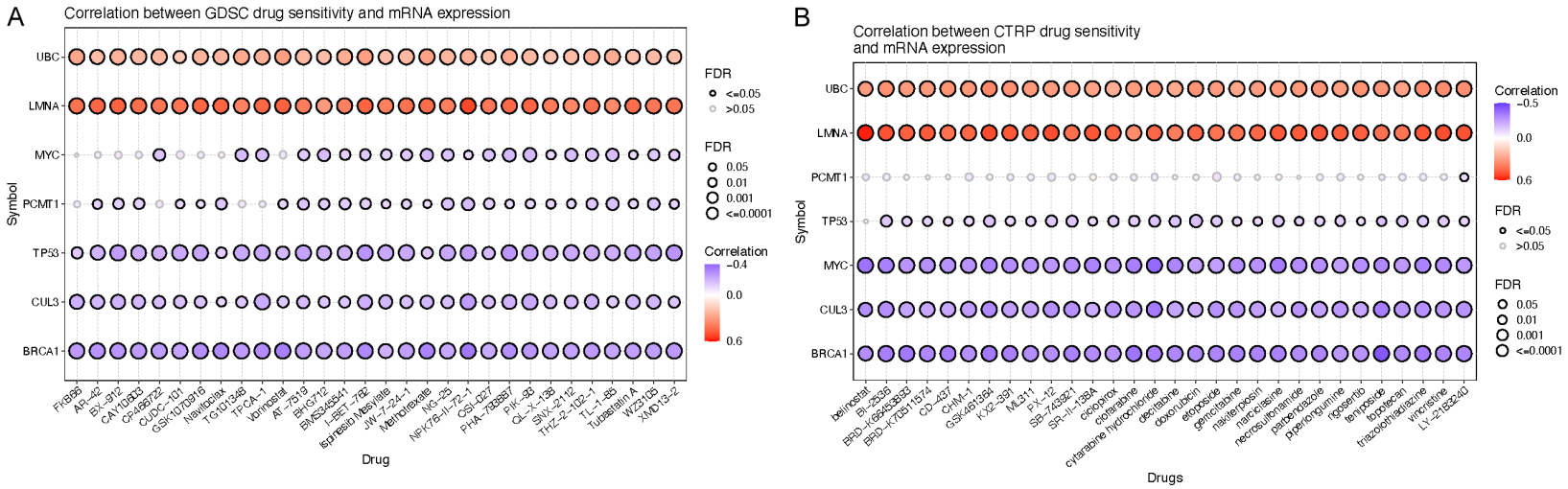

Figure 5. Correlation analysis of PCMT1 and drug susceptibility. A. Genomics of Drug Sensitivity in Cancer (GDSC). B. Cancer Therapeutics Response Portal (CTRP).

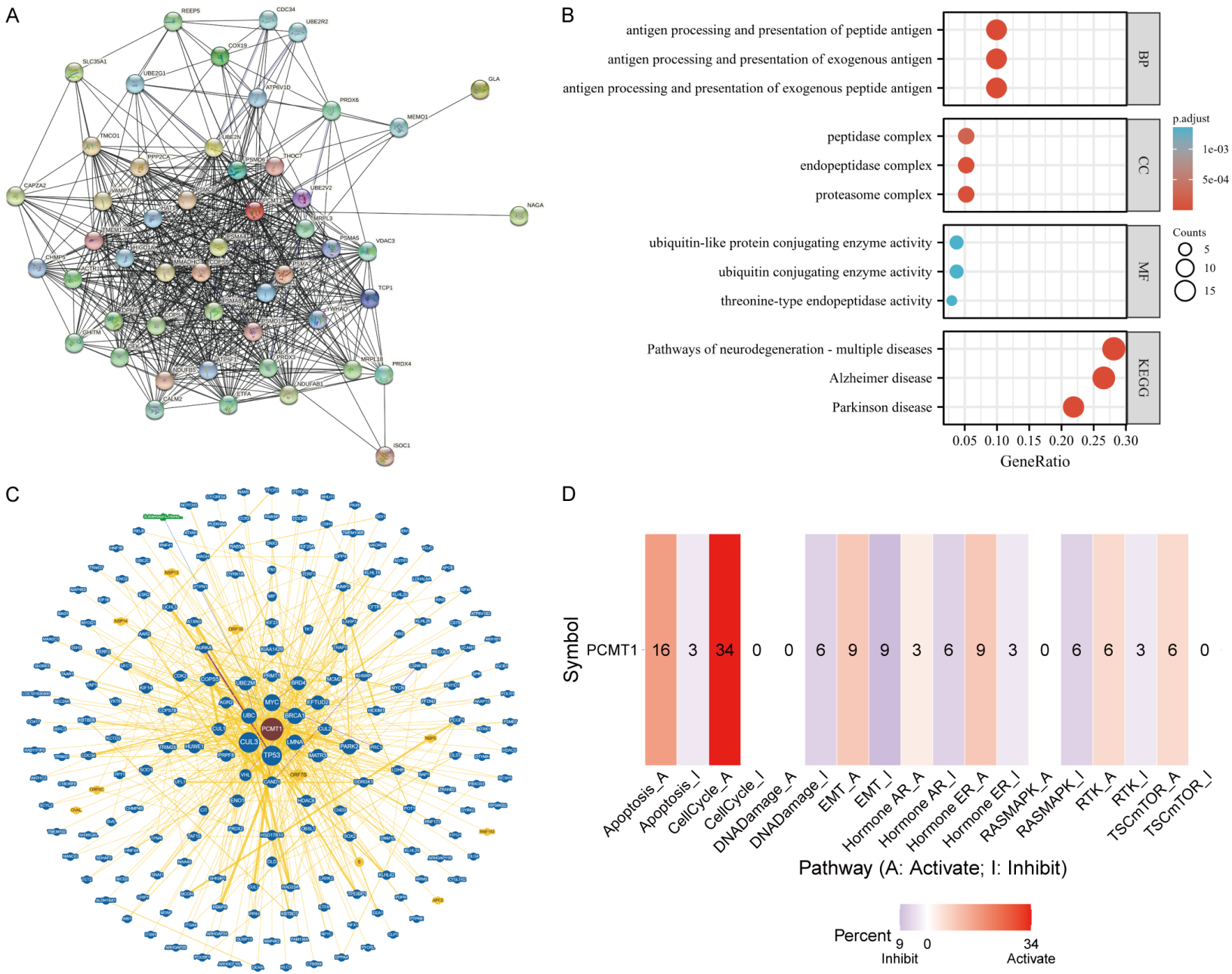
A
B
antigen processing and presentation of peptide antigen
antigen processing and presentation of exogenous antigen
antigen processing and presentation of exogenous peptide antigen
BP
peptidase complex
endopeptidase complex
proteasome complex
CC
ubiquitin-like protein conjugating enzyme activity
ubiquitin conjugating enzyme activity
threonine-type endopeptidase activity
MF
Pathways of neurodegeneration - multiple diseases
Alzheimer disease
Parkinson disease
KEGG
p.adjust
1e-03
5e-04
Counts
5
10
15
0.05 0.10 0.15 0.20 0.25 0.30
GeneRatio
C
D
Symbol
PCMT1 16 3 34 0 0 6 9 9 3 6 9 3 0 6 6 3 6 0
Apoptosis_A
Apoptosis_I
CellCycle_A
CellCycle_I
DNADamage_A
DNADamage_I
EMT_A
EMT_I
Hormone AR_A
Hormone AR_I
Hormone ER_A
Hormone ER_I
RASMAPK_A
RASMAPK_I
RTK_A
RTK_I
TSCmTOR_A
TSCmTOR_I
Pathway (A: Activate; I: Inhibit)
Percent
9 0 34
Inhibit
Activate

Figure 6. Functional enrichment analysis of PCMT1-related genes. A. The co-expression network consist of 50 binding proteins to PCMT1 through the STRING website. B. Gene Ontology (GO) analysis and Kyoto Gene and Genome (KEGG) analysis for 150 genes combinations with the most similar expression pattern to PCMT1 from STRING and GEPIA2. C. PCMT1-protein interactions obtained by BioGRID. D. Generalization of the impact of PCMT1 expression on the activity of 10 classical cancer pathways.

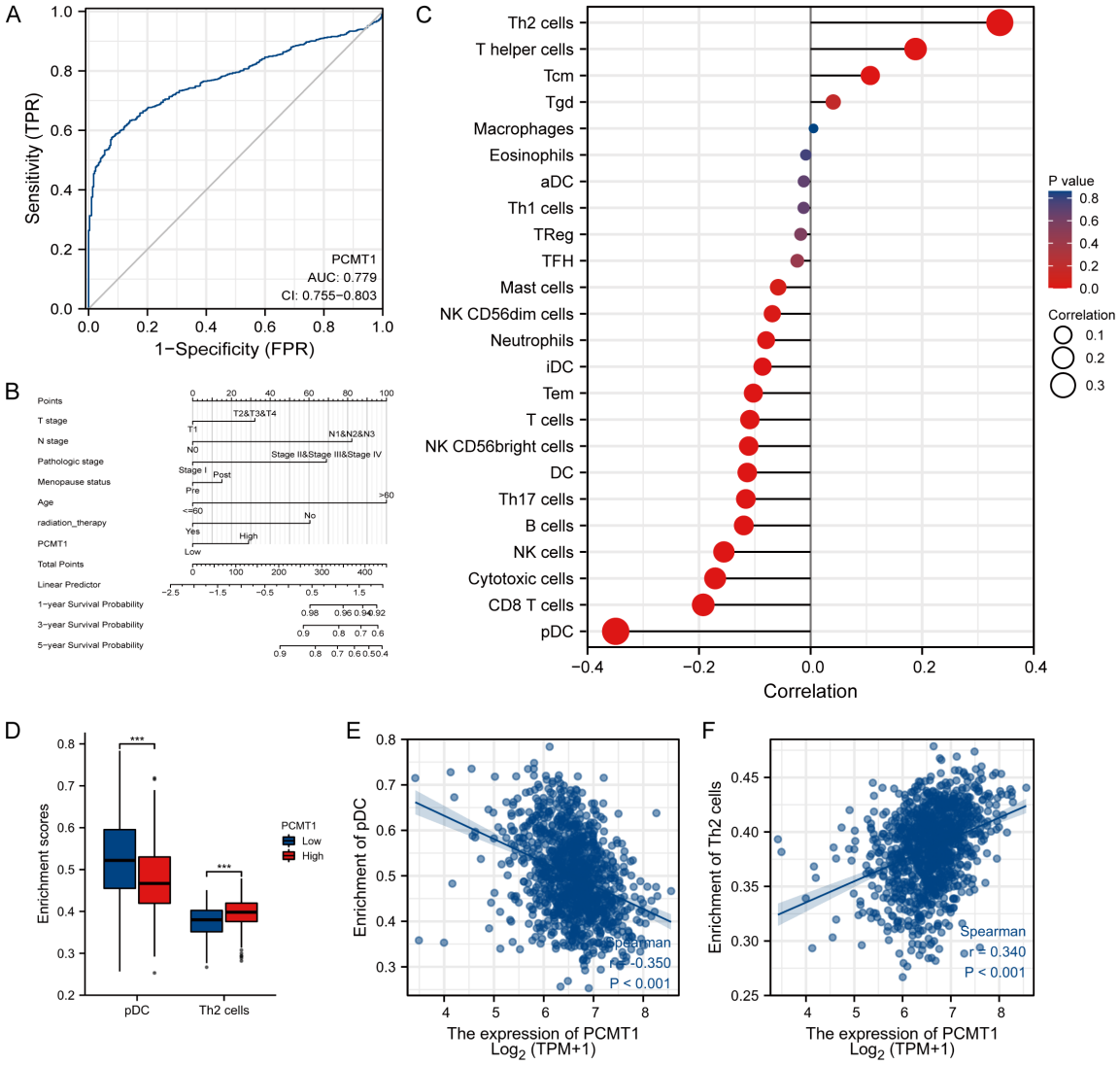

Figure 7. Clinical correlation and immune-related analyses of PCMT1 in BRCA. A. The receiver operating characteristic (ROC) curve of PCMT1. B. Prediction model of nomogram construction. C. The forest plot shows the correlation between PCMT1 expression level and 24 immune cells. The size of dots indicates the absolute value of Spearman r. D. The Wilcoxon rank sum test was used to analyze the difference of plasmacytoid pre-dendritic cells (pDC) and CD4+ T helper 2 (Th2) cells infiltration level between PCMT1 high and low expression groups. E. The correlation between PCMT1 expression and pDC was detected by Spearman correlation method. F. The correlation between PCMT1 expression and Th2 cells was detected by Spearman correlation method. *P<0.05; ***P<0.001.

PCMT1 regulates BC cell migration and invasion, yet displays no correlation with cell proliferation

Our investigation revealed that PCMT1 modulates BC cell migration and invasion, yet it does not influence cell proliferation. Notably, aberrant PCMT1 expression was significantly associated with BRCA prognosis, yet its precise role in BRCA development remains elusive. To elucidate the biological function of PCMT1 in BRCA, we analyzed its expression in five distinct BC

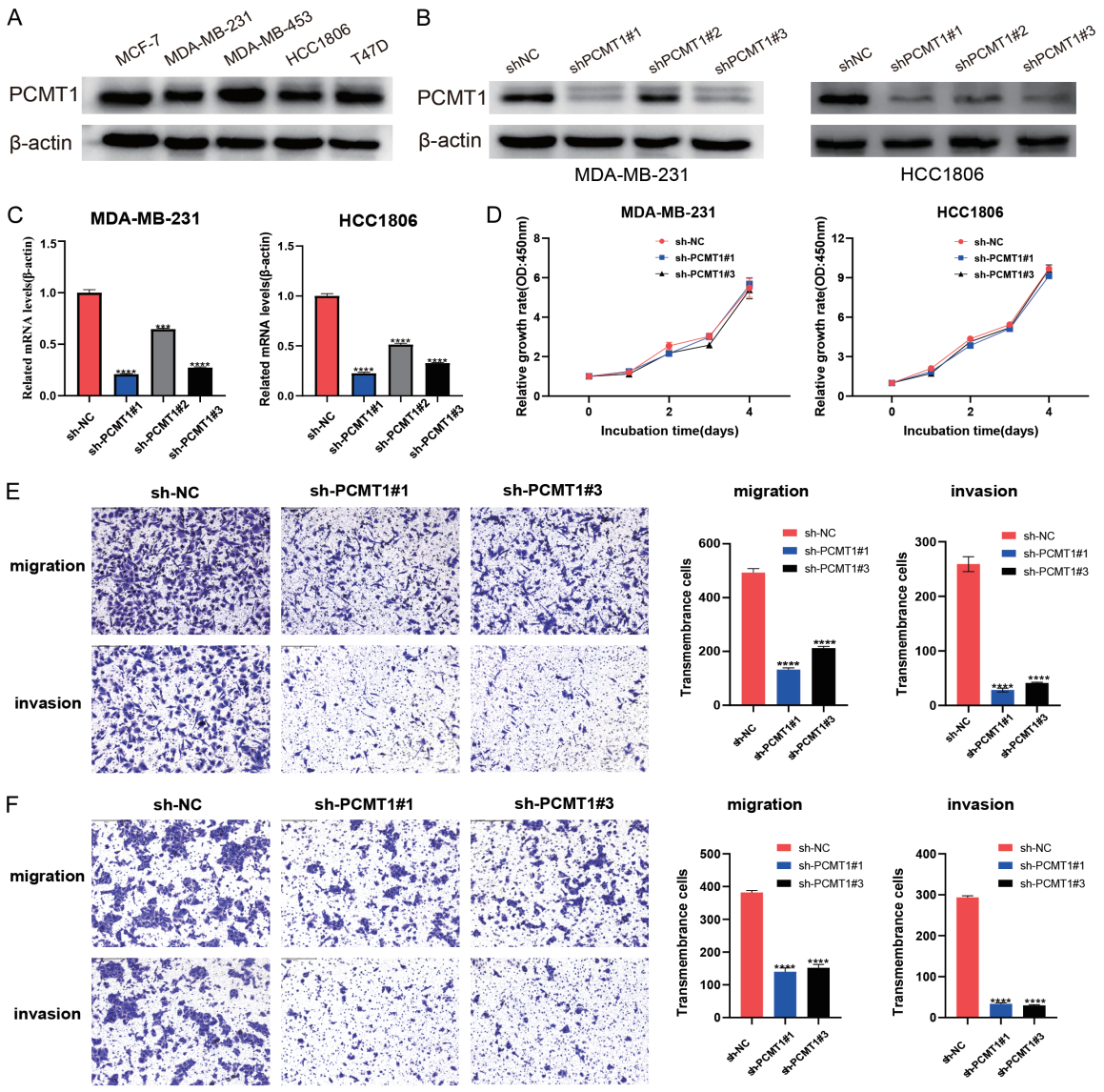

Figure 8. PCMT1 affects the migration and invasion ability of breast cancer cells. (A) Western blot analysis of PCMT1 protein expression in BRCA cell lines (MCF-7, MDA-MB-231, MDA-MB-453, HCC1806, T47D). Weston blot (B) and quantitative real-time PCR (C) were used to examine the knockdown efficiency of PCMT1 in MDA-MB-231 and HCC1806 cells. (D) Detection of proliferation of MDA-MB-231 and HCC1806 cells with the cell counting kit-8 (CCK-8). (E, F) Reducing PCMT1 expression can inhibit the migration and invasion of MDA-MB-231 and HCC1806 cells (original magnification, ×100; scale bars, 275 μm). The histogram showed the number of cells, and the cell counts were statistically analyzed. ***P<0.001; ****P<0.0001. BRCA: breast invasive carcinoma.

cell lines (MCF-7, MDA-MB-231, HCC1806, MDA-MB-453, T47D). Western blot analysis revealed high PCMT1 expression in all five cell types (**Figure 8A**). Based on this expression profile, we designed effective shRNAs to reduce PCMT1 expression in MDA-MB-231 and HCC1806 cells. Knockdown efficiency was validated using western blot (**Figure 8B**) and qRT-PCR (**Figure 8C**). The shRNA with the highest knockdown efficiency (shRNA-PCMT1#1) was chosen for further experiments. CCK-8 assays indicated that PCMT1 expression did not alter the proliferative capacity of MDA-MB-231 and HCC1806 cells (**Figure 8D**). To assess metastatic potential, cell migration and invasion assays were performed. Transwell assays revealed that downregulation of PCMT1 significantly reduced the migratory and invasive capabilities of MDA-MB-231 and HCC1806 cells (**Figure 8E**, **8F**).

PCMT1 modulated BC tumor growth and metastasis

In vitro experiments have established that PCMT1 regulates the migration and invasion of BC cells. To assess the impact of PCMT1 on tumor growth and metastasis in BRCA, we injected MDA-MB-231 and HCC1806 BC cells subcutaneously and intravenously into nude mice. Subcutaneous injection experiments demonstrated that reduced PCMT1 expression in these cells hindered tumor growth (refer to **Figure 9A-D**). HE staining revealed that PCMT1 inhibition induces vacuolar necrosis in tumor tissues (see **Figure 9E**, **9F**), while immunohistochemistry verified the effective knockdown of shRNA-PCMT1 in both cell lines (**Figure 9G-J**). However, intravenous injection of these cells into nude mice indicated that PCMT1 does not influence tumor metastasis in vivo (**Figure 9K**, **9L**).

Discussion

PIMT (gene name PCMT1) is a ubiquitous enzyme, yet most of its relevant investigations have been confined to non-oncological fields. Current studies exploring PCMT1's role in tumors are limited to a select few cancer types, leaving its pan-cancer influence elusive [32]. Herein, we present a comprehensive analysis of PCMT1's impact across various cancers. We systematically investigated PCMT1 expression in 33 human tumor types using TCGA and GTEx datasets, revealing its overexpression in most tumor tissues. Furthermore, we analyzed the prognostic value of PCMT1 in pan-cancer, encompassing OS, DFS, PFS, and DSS. Regarding OS, PCMT1 emerged as a risk factor in several cancer types, including bladder cancer BLCA, BRCA, HNSC, LIHC, LUAD, and MESO, while exhibiting a protective role in KIRC and READ. This finding aligns with previous studies reporting PCMT1's association with prognosis in cancers such as BLAC [17], LUAD [18], BC [19], and OC [20].

In our study, the findings revealed that both genetic variations and methylation of PCMT1 significantly impacted PCMT1 expression. Notably, genetic alterations played a role in tumor metastasis [33]. Previous research indicated that gene mutations could influence the prognosis and chemotherapy sensitivity of ovarian cancer [34]. DNA methylation is vital in cancer progression, regulating transcription in various cell types [35]. Our results showed a negative correlation between DNA methylation and PCMT1 expression in 32 tumor types, excluding THCA. Furthermore, we found that PCMT1's DNA methylation levels correlated with the prognosis of certain cancers.

TME comprises the cytological milieu where tumor or cancer stem cells reside, encompassing peripheral immune cells, vasculature, fibroblasts, extracellular matrix (ECM), lymphocytes, and signaling molecules [36-38]. Extensive research has linked the immunological cell infiltrate in the TME to tumor progression and prognosis [23, 39]. While PCMT1 has been significantly associated with immunological infiltrate in BC [19, 40], its relationship with tumor immunity in a pan-cancer context remains unexplored. In our study, PCMT1 displayed a positive correlation with common lymphoid progenitor and CD4(+) Th2 cells in several malignancies. Conversely, it exhibited a negative correlation with central and effector memory T cells, memory CD8(+) T cells, and CD4(+) Th1 cells. Cytokines produced by CD4+ Th1 cells, such as IL-1β, IL-2, IL-12, TNF-α, and IFN-γ, are associated with favorable prognosis in hepatocellular carcinoma patients [41]. In contrast, cytokines secreted by CD4+ Th2 cells, including IL-4, IL-5, and IL-10, are linked to tumor growth or metastasis [42]. Memory CD8(+) T cells improve tumor prognosis by activating an immune response against tumor cells, recognizing specific antigens [43, 44]. Furthermore, CD4+ Th1 cells support CD8+ T cells by releasing IFN-γ and IL-2 [45]. Based on these findings, we hypothesize that PCMT1 may contribute to tumor development by modulating the balance between Th1, Th2, and CD8+ memory T cells. The variability in the relationship between PCMT1 and tumor immunity across different tumor types could explain the diverse prognostic roles of PCMT1 expression.

Tumor therapeutic resistance remains a critical challenge in modern oncology. The development of drug resistance in tumors is multifaceted, encompassing local immunosuppression, tolerance induction, and systemic T-cell signaling malfunctions [46-49]. To combat this, tumors utilize diverse evasion mechanisms like immunological editing, immune deviation, and altered antigen presentation [50], necessitating the development of novel ICI therapies.

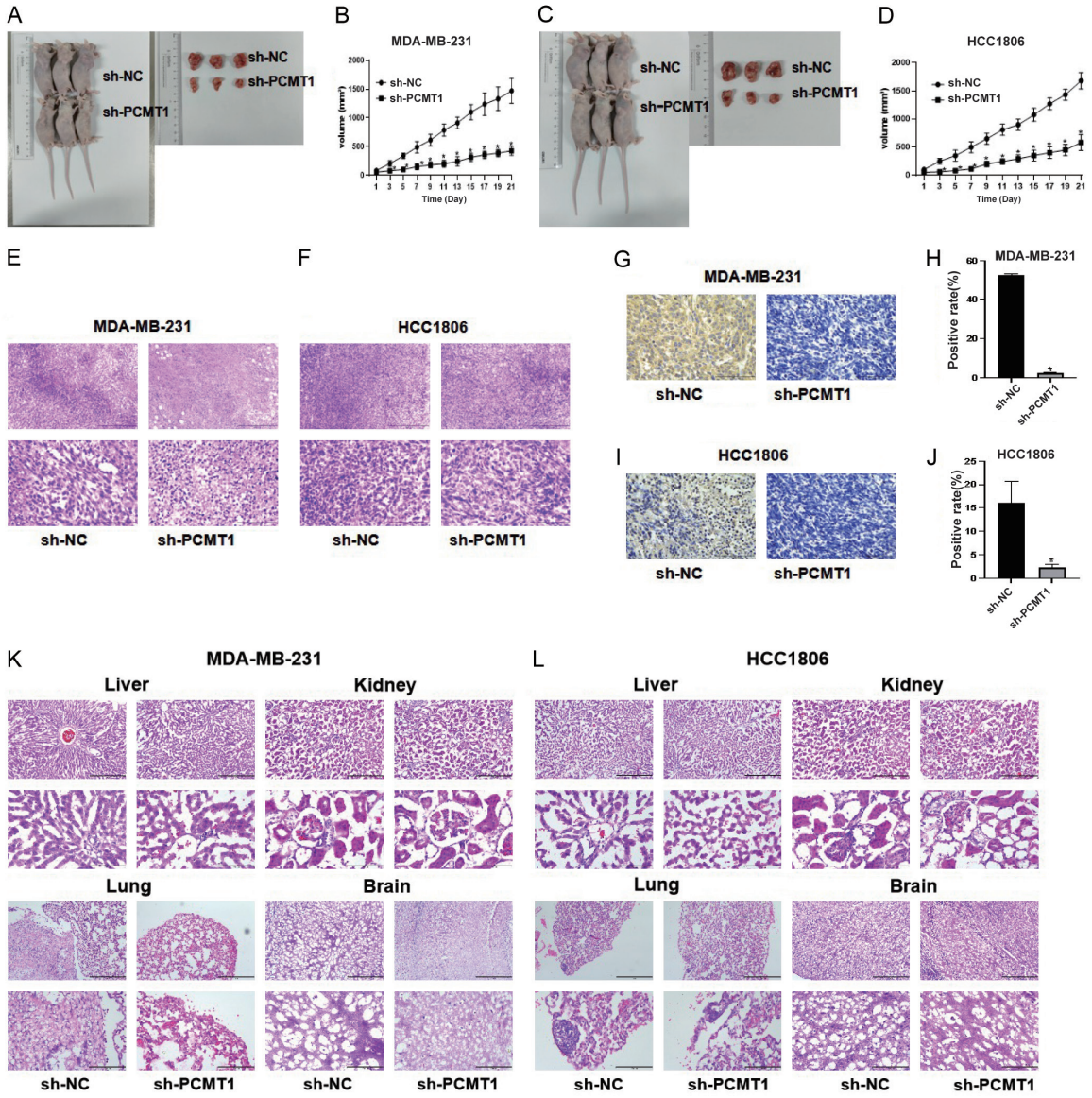

Figure 9. PCMT1 affects the tumor growth and metastasis of breast cancer cells. A-D. Tumor growth. E, F. Tumor tissues (original magnification, ×100, ×200; scale bars, 400 μm, 100 μm). G-J. PCMT1 positive expression (original magnification, ×200; scale bars, 100 μm). K, L. Tumor metastasis (original magnification, ×100, ×200; scale bars, 400 μm, 100 μm). *P<0.05.

In recent decades, neutralizing antibodies targeting immunological checkpoints, such as T-lymphocyte-associated protein 4 (CTLA-4) and programmed cell death protein 1 (PD-1), have demonstrated promising therapeutic outcomes [51]. However, the mainstream adoption of immunotherapy has been significantly hindered by low objective response rates, unique immune-related toxicities, hyperprogression, and the absence of reliable predictive markers for treatment efficacy [52]. Furthermore, therapeutic combinations can optimize clinical efficacy. For example, combination therapy targeting both CTLA-4 and PD-1 has significantly improved median survival rates across various tumor types [53]. Currently, TMB [28] and MSI [29] are regarded as potential biomarkers for predicting the effectiveness of tumor immunotherapy. Therefore, combining these biomarkers could enhance the predictive accuracy of ICIs, facilitating better treatment selection. This study explores the comprehensive correlation between PCMT1 expression and response to ICIs biomarkers,

focusing on immunological checkpoint-associated genes, TMB, and MSI. Our findings reveal a strong association between PCMT1 expression and the presence of 8 immunological checkpoints (CD274, LAG3, HAVCR2, SIGLEC-15, CTLA4, PDCD1, PDCD1LG2, and TIGIT) across multiple tumor types. Additionally, we investigated the relationship between PCMT1 expression and both TMB and MSI in a pan-cancer analysis. Positive correlations between PCMT1 expression and TMB were observed in ACC, BRCA, LUAD, SKCM, and STAD, whereas negative correlations were found in HNSC, THCA, and THYM. Moreover, PCMT1 expression demonstrated positive correlations with MSI in KIRC, STAD, and UCEC, and negative associations in CHOL, LUAD, PCPG, and PRAD. These results suggest that PCMT1 could serve as a predictor for specific malignancies' response to ICIs.

To investigate the potential role of PCMT1 in tumors, we utilized STRING and GEPIA2 to identify 150 genes that are co-expressed with PCMT1 and subsequently performed functional enrichment analyses. KEGG pathway analysis revealed that PCMT1 may function through pathways associated with Alzheimer's disease, Parkinson's disease, and neurodegenerative disorders, consistent with previous studies demonstrating PCMT1's involvement in various CNS diseases, including Alzheimer's disease [9], Parkinson's syndrome [10], and multiple sclerosis [11]. In the PCMT1-protein interaction network, TP53, CUL3, BRCA1, LMNA, MYC, and UBC emerged as the most closely associated proteins. Notably, previous research has shown that PCMT1 can inhibit the oncogenic effects of P53 by modulating its expression, thereby suppressing tumor apoptosis [54]. Furthermore, our study analyzed the association between PCMT1 and 10 well-known cancer-related pathways. The results indicated that PCMT1 is strongly linked to apoptosis, cell cycle, and EMT pathways. While EMT is crucial for normal embryogenesis, it plays a pivotal role in promoting malignancy development and metastasis [55]. By regulating the expression of EMT-related genes, PCMT1 has been shown to influence bladder cancer migration and invasion [17].

In this bioinformatics analysis, PCMT1 was found to exhibit aberrantly elevated expression in BRCA and was significantly associated with BRCA prognosis, serving as an independent prognostic factor. Additionally, our research validated the high expression of PCMT1 in BRCA cell lines. To further elucidate the role of PCMT1 in BRCA development, we engineered lentiviruses to knockdown PCMT1 expression. The results revealed that reducing PCMT1 expression inhibited breast cancer cell migration and invasion, while having no significant impact on cell proliferation. This study has significantly advanced our understanding of the relationship between PCMT1 and human cancer. However, there are some limitations that should be noted. Firstly, this research relied on a retrospective analysis of the data. Secondly, the relatively small sample size for some less common tumor types may have led to potential inaccuracies in the results. Future studies with larger and more diverse sample sizes are needed to validate our findings.

In conclusion, PCMT1 expression is aberrantly upregulated in numerous tumor tissues, and this upregulation is closely associated with tumor prognosis. Moreover, PCMT1 was strongly correlated with tumor immunity and response to ICIs, suggesting that PCMT1 may serve as a potential immunotherapeutic target for guiding personalized cancer immunotherapy. Furthermore, our findings demonstrate that PCMT1 knockdown suppresses BC invasion and migration, highlighting PCMT1's potential as a diagnostic and prognostic biomarker.

Acknowledgements

This work was supported by grants from the Natural Science Foundation of Hunan Province (No. 2019JJ20014), and the National Natural Science Foundation of China (Nos. 81372824, 81773294).

Disclosure of conflict of interest

None.

Address correspondence to: Renxian Cao and Jing Zhong, Institute of Clinical Medicine, The First Affiliated Hospital, Hengyang Medical School, University of South China, No. 69 Chuanshan Avenue, Shigu District, Hengyang 421200, Hunan, China. Tel: +86-0734-8279467; E-mail: caorenxian@hotmail.com (RXC); zhongjing2002@usc.edu.cn (JZ)

References

[1] Siegel RL, Miller KD, Fuchs HE and Jemal A. Cancer statistics, 2022. CA Cancer J Clin 2022; 72: 7-33.

[2] Sung H, Ferlay J, Siegel RL, Laversanne M, Soerjomataram I, Jemal A and Bray F. Global cancer statistics 2020: GLOBOCAN estimates of incidence and mortality worldwide for 36 cancers in 185 countries. CA Cancer J Clin 2021; 71: 209-249.

[3] Santucci C, Carioli G, Bertuccio P, Malvezzi M, Pastorino U, Boffetta P, Negri E, Bosetti C and La Vecchia C. Progress in cancer mortality, incidence, and survival: a global overview. Eur J Cancer Prev 2020; 29: 367-381.

[4] Zhang Y and Zhang Z. The history and advances in cancer immunotherapy: understanding the characteristics of tumor-infiltrating immune cells and their therapeutic implications. Cell Mol Immunol 2020; 17: 807-821.

[5] Desrosiers RR and Fanélus I. Damaged proteins bearing L-isoaspartyl residues and aging: a dynamic equilibrium between generation of isomerized forms and repair by PIMT. Curr Aging Sci 2011; 4: 8-18.

[6] Simko V, Belvoncikova P, Csaderova L, Labudova M, Grossmannova K, Zatovicova M, Kajanova I, Skultety L, Barathova M and Pastorek J. PIMT binding to C-terminal Ala459 of CAIX is involved in inside-out signaling necessary for its catalytic activity. Int J Mol Sci 2020; 21: 8545.

[7] Boivin D, Bilodeau D and Béliveau R. Immunochemical characterization of L-isoaspartyl-protein carboxyl methyltransferase from mammalian tissues. Biochem J 1995; 309: 993-998.

[8] Qin Z, Yang J, Klassen HJ and Aswad DW. Isoaspartyl protein damage and repair in mouse retina. Invest Ophthalmol Vis Sci 2014; 55: 1572-1579.

[9] Bae N, Byeon SE, Song J, Lee SJ, Kwon M, Mook-Jung I, Cho JY and Hong S. Knock-down of protein L-isoaspartyl O-methyltransferase increases β-amyloid production by decreasing ADAM10 and ADAM17 levels. Acta Pharmacol Sin 2011; 32: 288-294.

[10] Ouazia D, Levros LC Jr, Rassart É and Desrosiers RR. The protein l-isoaspartyl (d-aspartyl) methyltransferase protects against dopamine-induced apoptosis in neuroblastoma SH-SY5Y cells. Neuroscience 2015; 295: 139-50.

[11] Friedrich MG, Hancock SE, Raftery MJ and Truscott RJ. Isoaspartic acid is present at specific sites in myelin basic protein from multiple sclerosis patients: could this represent a trigger for disease onset? Acta Neuropathol Commun 2016; 4: 83.

[12] DeVry CG and Clarke S. Polymorphic forms of the protein L-isoaspartate (D-aspartate) O-methyltransferase involved in the repair of age-damaged proteins. J Hum Genet 1999; 44: 275-88.

[13] Pyun JA, Kang H, Lee SK, Kim MH and Kwack K. Association between polymorphisms in the protein L-isoaspartate (D-aspartate) O-methyltransferase gene and premature ovarian failure. Fertil Steril 2009; 91 Suppl: 1362-5.

[14] Jia Y, Liu N, Viswakarma N, Sun R, Schipma MJ, Shang M, Thorp EB, Kanwar YS, Thimmapaya B and Reddy JK. PIMT/NCOA6IP deletion in the mouse heart causes delayed cardiomyopathy attributable to perturbation in energy metabolism. Int J Mol Sci 2018; 19: 1485.

[15] Yang H, Lowenson JD, Clarke S and Zubarev RA. Brain proteomics supports the role of glutamate metabolism and suggests other metabolic alterations in protein l-isoaspartyl methyltransferase (PIMT)-knockout mice. J Proteome Res 2013; 12: 4566-4576.

[16] Kapadia B, Viswakarma N, Parsa KV, Kain V, Behera S, Suraj SK, Babu PP, Kar A, Panda S, Zhu YJ, Jia Y, Thimmapaya B, Reddy JK and Misra P. ERK2-mediated phosphorylation of transcriptional coactivator binding protein PIMT/NCoA6IP at Ser298 augments hepatic gluconeogenesis. PLoS One 2013; 8: e83787.

[17] Dong L, Li Y, Xue D and Liu Y. PCMT1 is an unfavorable predictor and functions as an oncogene in bladder cancer. IUBMB Life 2018; 70: 291-299.

[18] Saito H, Yamashita M, Ogasawara M, Yamada N, Niisato M, Tomoyasu M, Deguchi H, Tanita T, Ishida K, Sugai T and Yamauchi K. Chaperone protein L-isoaspartate (D-aspartyl) O-methyltransferase as a novel predictor of poor prognosis in lung adenocarcinoma. Hum Pathol 2016; 50: 1-10.

[19] Guo J, Du X and Li C. PCMT1 is a potential prognostic biomarker and is correlated with immune infiltrates in breast cancer. Biomed Res Int 2022; 2022: 4434887.

[20] Zhang J, Li Y, Liu H, Zhang J, Wang J, Xia J, Zhang Y, Yu X, Ma J, Huang M, Wang J, Wang L, Li Q, Cui R, Yang W, Xu Y and Feng W. Genome-wide CRISPR/Cas9 library screen identifies PCMT1 as a critical driver of ovarian cancer metastasis. J Exp Clin Cancer Res 2022; 41: 24.

[21] Ouazia D, Levros LC Jr, Rassart E and Desrosiers RR. Dopamine down-regulation of protein L-isoaspartyl methyltransferase is dependent on reactive oxygen species in SH-SY5Y cells. Neuroscience 2014; 267: 263-76.

[22] Ouanouki A and Desrosiers RR. The enzyme L-isoaspartyl (D-aspartyl) methyltransferase is required for VEGF-dependent endothelial cell

migration and tubulogenesis. Mol Cell Biochem 2016; 413: 37-46.
[23] Engelhard VH, Rodriguez AB, Mauldin IS, Woods AN, Peske JD and Slingluff CL Jr. Immune cell infiltration and tertiary lymphoid structures as determinants of antitumor immunity. J Immunol 2018; 200: 432-442.
[24] Sturm G, Finotello F, Petitprez F, Zhang JD, Baumbach J, Fridman WH, List M and Aneichyk T. Comprehensive evaluation of transcriptome-based cell-type quantification methods for immuno-oncology. Bioinformatics 2019; 35: i436-i445.
[25] Bagchi S, Yuan R and Engleman EG. Immune checkpoint inhibitors for the treatment of cancer: clinical impact and mechanisms of response and resistance. Annu Rev Pathol 2021; 16: 223-249.
[26] Addeo A, Friedlaender A, Banna GL and Weiss GJ. TMB or not TMB as a biomarker: that is the question. Crit Rev Oncol Hematol 2021; 163: 103374.
[27] Bonneville R, Krook MA, Kautto EA, Miya J, Wing MR, Chen HZ, Reeser JW, Yu L and Roychowdhury S. Landscape of microsatellite instability across 39 cancer types. JCO Precis Oncol 2017; 2017: PO.17.00073.
[28] Chan TA, Yarchoan M, Jaffee E, Swanton C, Quezada SA, Stenzinger A and Peters S. Development of tumor mutation burden as an immunotherapy biomarker: utility for the oncology clinic. Ann Oncol 2019; 30: 44-56.
[29] van Velzen MJM, Derks S, van Grieken NCT, Haj Mohammad N and van Laarhoven HWM. MSI as a predictive factor for treatment outcome of gastroesophageal adenocarcinoma. Cancer Treat Rev 2020; 86: 102024.
[30] Yu G, Wang LG, Han Y and He QY. clusterProfiler: an R package for comparing biological themes among gene clusters. OMICS 2012; 16: 284-287.
[31] Bindea G, Mlecnik B, Tosolini M, Kirilovsky A, Waldner M, Obenauf AC, Angell H, Fredriksen T, Lafontaine L, Berger A, Bruneval P, Fridman WH, Becker C, Pagès F, Speicher MR, Trajanoski Z and Galon J. Spatiotemporal dynamics of intratumoral immune cells reveal the immune landscape in human cancer. Immunity 2013; 39: 782-795.
[32] Edwin RK, Challa N, Sharma R, Satyamoorthy K, Parsa K and Misra P. PIMT/TGS1: an evolving metabolic molecular switch with conserved methyl transferase activity. Drug Discov Today 2022; 27: 2386-2393.
[33] Cha S, Lee E and Won HH. Comprehensive characterization of distinct genetic alterations in metastatic breast cancer across various metastatic sites. NPJ Breast Cancer 2021; 7: 93.
[34] Yang D, Khan S, Sun Y, Hess K, Shmulevich I, Sood AK and Zhang W. Association of BRCA1 and BRCA2 mutations with survival, chemotherapy sensitivity, and gene mutator phenotype in patients with ovarian cancer. JAMA 2011; 306: 1557-65.
[35] Mehdi A and Rabbani SA. Role of methylation in pro- and anti-cancer immunity. Cancers (Basel) 2021; 13: 545.
[36] Trepel J, Mollapour M, Giaccone G and Neckers L. Targeting the dynamic HSP90 complex in cancer. Nat Rev Cancer 2010; 10: 537-549.
[37] Arneth B. Tumor microenvironment. Medicina (Kaunas) 2019; 56: 15.
[38] Shelton LB, Baker JD, Zheng D, Sullivan LE, Solanki PK, Webster JM, Sun Z, Sabbagh JJ, Nordhues BA, Koren J 3rd, Ghosh S, Blagg BSJ, Blair LJ and Dickey CA. Hsp90 activator Aha1 drives production of pathological tau aggregates. Proc Natl Acad Sci U S A 2017; 114: 9707-9712.
[39] Huntington ND, Cursons J and Rautela J. The cancer-natural killer cell immunity cycle. Nat Rev Cancer 2020; 20: 437-454.
[40] Lv W, Zhao C, Tan Y, Hu W, Yu H, Zeng N, Zhang Q and Wu Y. Identification of an aging-related gene signature in predicting prognosis and indicating tumor immune microenvironment in breast cancer. Front Oncol 2021; 11: 796555.
[41] Budhu A, Forgues M, Ye QH, Jia HL, He P, Zanetti KA, Kammula US, Chen Y, Qin LX, Tang ZY and Wang XW. Prediction of venous metastases, recurrence, and prognosis in hepatocellular carcinoma based on a unique immune response signature of the liver microenvironment. Cancer Cell 2006; 10: 99-111.
[42] Mantovani A, Allavena P, Sica A and Balkwill F. Cancer-related inflammation. Nature 2008; 454: 436-44.
[43] Hivroz C, Chemin K, Tourret M and Bohineust A. Crosstalk between T lymphocytes and dendritic cells. Crit Rev Immunol 2012; 32: 139-55.
[44] Klebanoff CA, Gattinoni L and Restifo NP. CD8+ T-cell memory in tumor immunology and immunotherapy. Immunol Rev 2006; 211: 214-24.
[45] Wang T, Niu G, Kortylewski M, Burdelya L, Shain K, Zhang S, Bhattacharya R, Gabrilovich D, Heller R, Coppola D, Dalton W, Jove R, Pardoll D and Yu H. Regulation of the innate and adaptive immune responses by Stat-3 signaling in tumor cells. Nat Med 2004; 10: 48-54.
[46] Topalian SL, Weiner GJ and Pardoll DM. Cancer immunotherapy comes of age. J Clin Oncol 2011; 29: 4828-4836.
[47] Mellman I, Coukos G and Dranoff G. Cancer immunotherapy comes of age. Nature 2011; 480: 480-489.

[48] Drake CG, Jaffee E and Pardoll DM. Mechanisms of immune evasion by tumors. Adv Immunol 2006; 90: 51-81.
[49] Mizoguchi H, O'Shea JJ, Longo DL, Loeffler CM, McVicar DW and Ochoa AC. Alterations in signal transduction molecules in T lymphocytes from tumor-bearing mice. Science 1992; 258: 1795-1798.
[50] Vinay DS, Ryan EP, Pawelec G, Talib WH, Stagg J, Elkord E, Lichtor T, Decker WK, Whelan RL, Kumara HMCS, Signori E, Honoki K, Georgakilas AG, Amin A, Helferich WG, Boosani CS, Guha G, Ciriolo MR, Chen S, Mohammed SI, Azmi AS, Keith WN, Bilsland A, Bhakta D, Halicka D, Fujii H, Aquilano K, Ashraf SS, Nowsheen S, Yang X, Choi BK and Kwon BS. Immune evasion in cancer: mechanistic basis and therapeutic strategies. Semin Cancer Biol 2015; 35 Suppl: S185-S198.
[51] Seidel JA, Otsuka A and Kabashima K. Anti-PD-1 and anti-CTLA-4 therapies in cancer: mechanisms of action, efficacy, and limitations. Front Oncol 2018; 8: 86.
[52] Hegde PS and Chen DS. Top 10 challenges in cancer immunotherapy. Immunity 2020; 52: 17-35.
[53] Rotte A. Combination of CTLA-4 and PD-1 blockers for treatment of cancer. J Exp Clin Cancer Res 2019; 38: 255.
[54] Lee JC, Kang SU, Jeon Y, Park JW, You JS, Ha SW, Bae N, Lubec G, Kwon SH, Lee JS, Cho EJ and Han JW. Protein L-isoaspartyl methyltransferase regulates p53 activity. Nat Commun 2012; 3: 927.
[55] Lu W and Kang Y. Epithelial-mesenchymal plasticity in cancer progression and metastasis. Dev Cell 2019; 49: 361-374.

Supplementary Table 1. Primers for qRT-PCR analysis and shRNA sequence targeting PCMT1

Name	Sequences (5'-3')
RT-qPCR primers	
PCMT1	F: CGCTGAAGGTGGTTCTGT; R: CATAGTGGGAGCGGTCTG
β-actin	F: CCTGGCACCCAGCACAAT; R: GGGCCGGACTCGTCATAC
shRNA sequences	
sh-PCMT1 #1	CAGTATGACAAGCTACAAGAT
sh-PCMT1 #2	CCAGGCGCTAATAGATCAGTT
sh-PCMT1 #3	GATCACATTAAAGAGCTAGTA
sh-NC	TTCTCCGAACGTGTCACGT

RT-qPCR: quantitative real-time reverse transcription polymerase chain reaction, shRNA: small interfering RNA, F: forward primer, R: reverse primer.

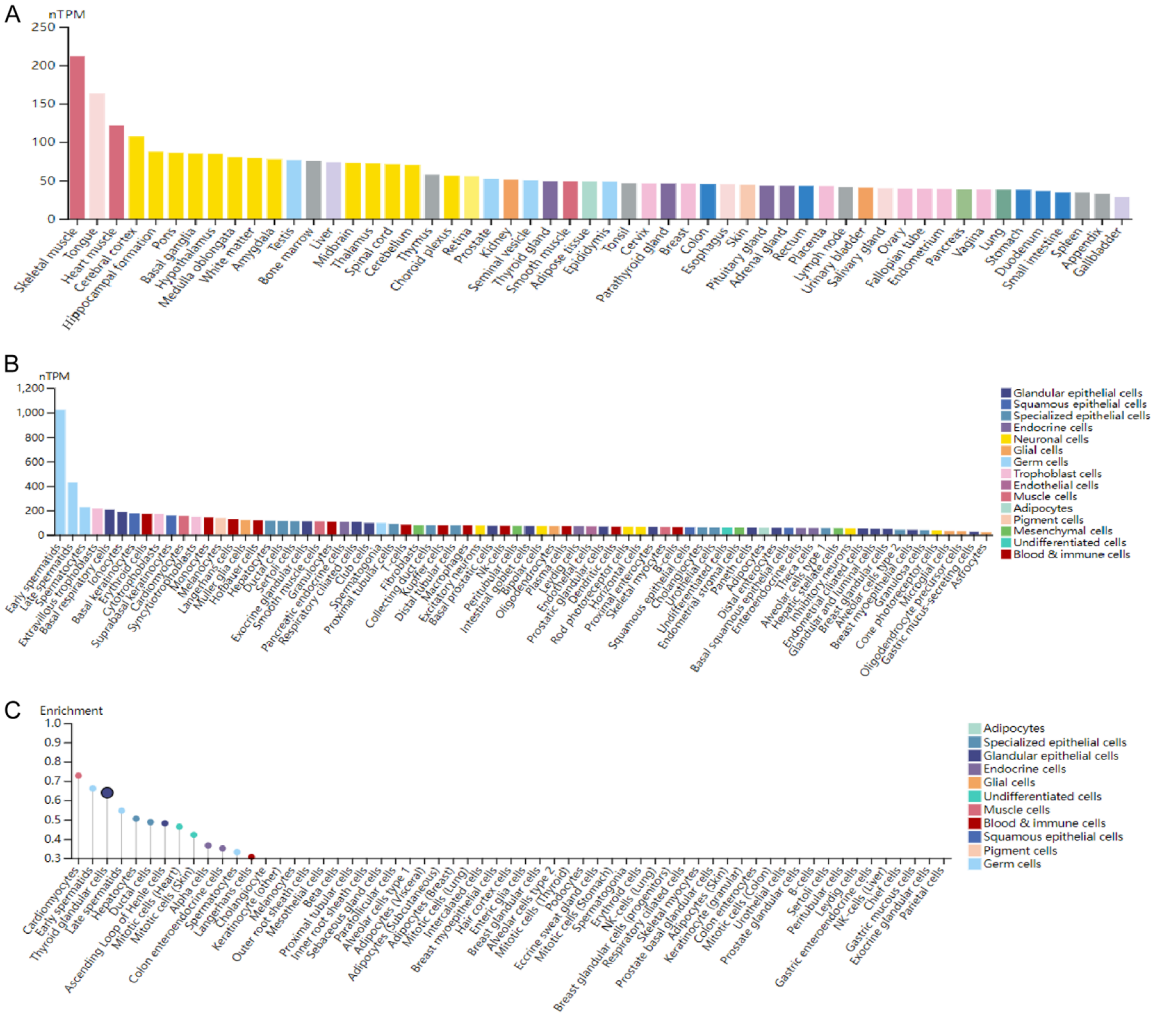

Supplementary Figure 1. Expression of PCMT1 mRNA in human cells and tissues. A. PCMT1 mRNA expression in different tissues from the consensus dataset, which consists of the HPA transcriptomics and the GTEx transcriptomics datasets. B. PCMT1 mRNA expression in different single cell types from the HPA database. C. PCMT1 mRNA expression in different tissue specific cell types from the HPA database.

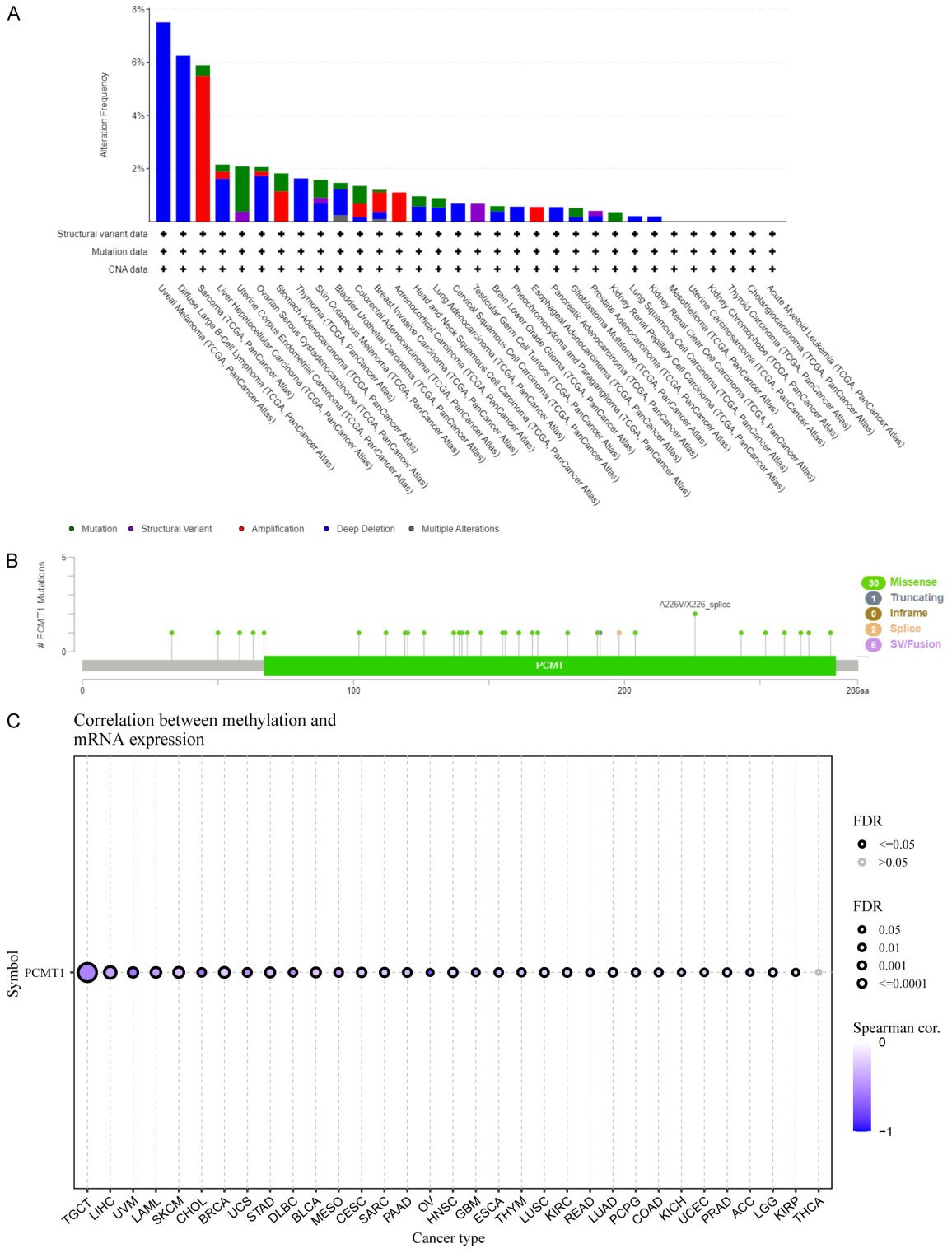

Supplementary Figure 2. Genetic alteration and DNA methylation of PCMT1 in various tumor types of TCGA. A. Mutation type summary of PCMT1 with its allocation in various cancers. B. Mutation site status of PCMT1. C. Correlation between DNA methylation levels and PCMT1 expression in multiple tumors.

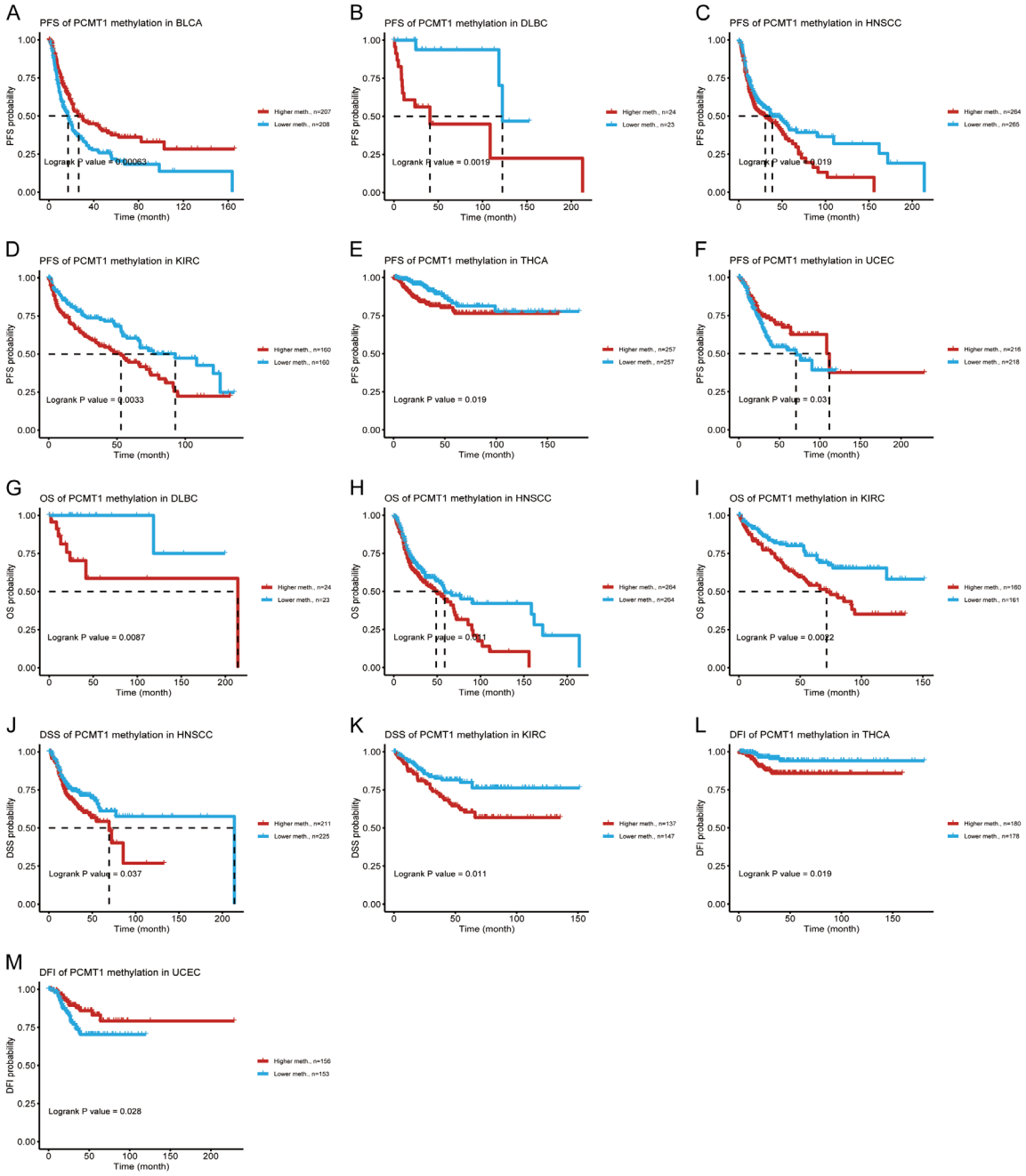

Supplementary Figure 3. Association between the PCMT1 methylation level and the disease-free survival patients (PFS) with various cancer patients. A. BLCA. B. DLBC. C. HNSCC. D. KIRC. E. THCA. F. UCEC. Association between the PCMT1 methylation level and the overall survival (OS) with various cancer patients. G. DLBC. H. HNSCC. I. KIRC. Association between the PCMT1 methylation level and the disease specific survival (DSS) with various cancer patients. J. HNSCC. K. KIRC. Association between the PCMT1 methylation level and the disease-free interval patients (DFI) with various cancer patients. L. THCA. M. UCEC. BLCA: bladder cancer, DLBC: diffuse large B-cell lymphoma, HNSCC: head and neck squamous cell carcinoma, KIRC: carcinoma, THCA: thyroid carcinoma, UCEC: uterine corpus endometrial carcinoma.

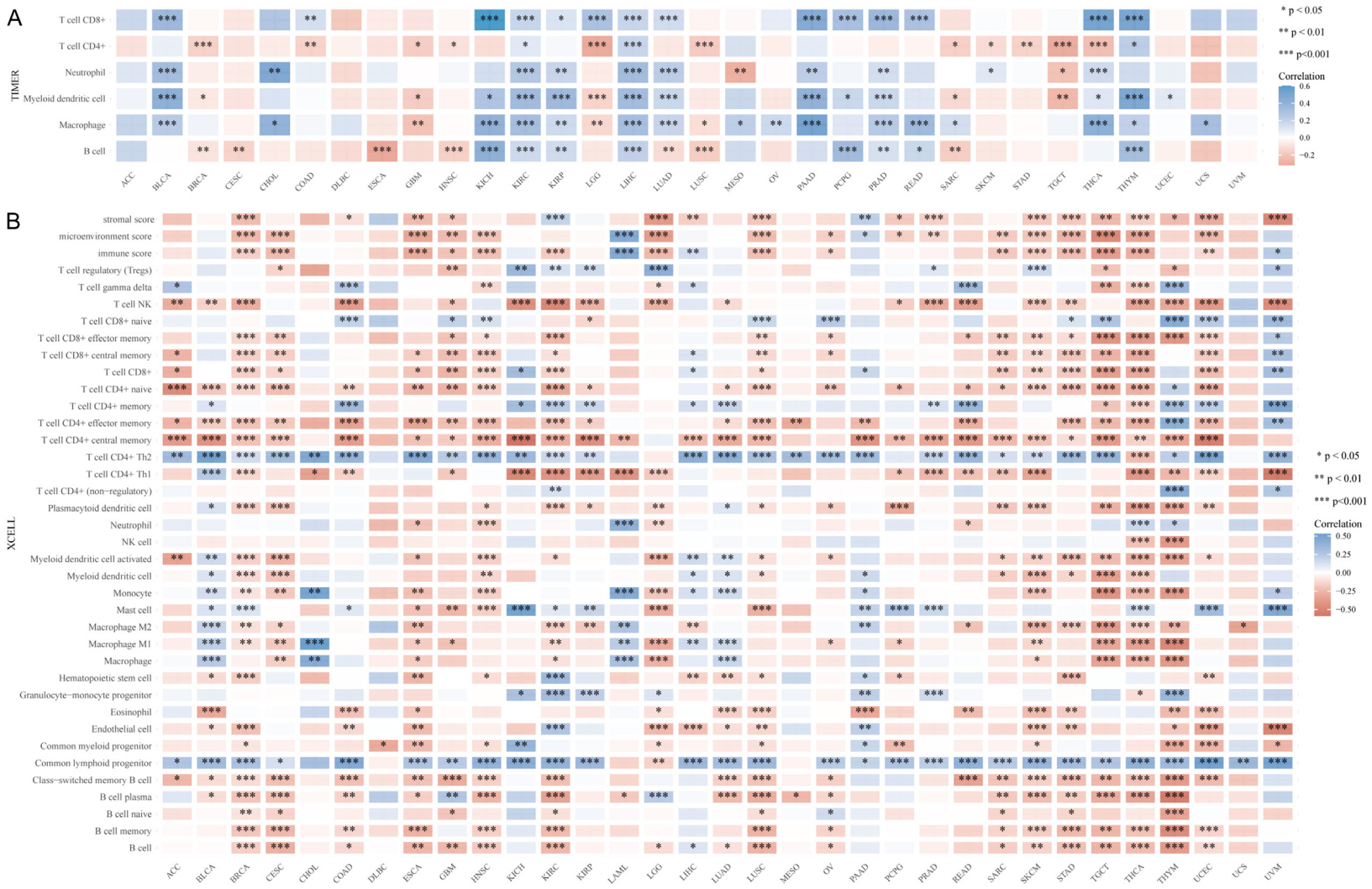

Supplementary Figure 4. Correlation of PCMT1 with immune infiltrating cells in pan-cancer based on different algorithms. A. Correlation of PCMT1 expression with the proportion of 6 immune infiltrating cells using the TIMER algorithm. B. Analyzed of the correlation between the expression of PCMT1 and the proportion of 38 immune infiltrating cells using the XCELL algorithm. *P<0.05; **P<0.01; ***P<0.001.

Supplementary Table 2. Univariate and multivariate Cox regression analyses of various factors on overall survival in BRCA

Characteristics	Total (N)	Univariate analysis		Multivariate analysis	
		Hazard ratio (95% CI)	*P* value	Hazard ratio (95% CI)	*P* value
T stage (T2 & T3 & T4 vs. T1)	1,079	1.482 (1.007-2.182)	0.046	1.139 (0.525-2.469)	0.743
N stage (N1 & N2 & N3 vs. N0)	1,063	2.239 (1.567-3.199)	<0.001	0.922 (0.365-2.332)	0.864
ERBB2 (High vs. Low)	1,082	0.966 (0.702-1.328)	0.830		
TP53 (High vs. Low)	1,082	1.360 (0.986-1.875)	0.061	1.060 (0.572-1.966)	0.854
Pathologic stage (Stage III & Stage IV vs. Stage I & Stage II)	1,059	2.391 (1.703-3.355)	<0.001	5.607 (2.229-14.103)	<0.001
ER status (Positive vs. Negative)	1,032	0.712 (0.495-1.023)	0.066	0.638 (0.247-1.649)	0.354
PR status (Positive vs. Negative)	1,029	0.732 (0.523-1.024)	0.068	0.620 (0.266-1.446)	0.268
HER2 status (Positive vs. Negative)	715	1.593 (0.973-2.609)	0.064	0.918 (0.439-1.919)	0.820
Menopause status (Post vs. Pre)	931	2.165 (1.302-3.600)	0.003	3.447 (1.205-9.856)	0.021
Age (>60 vs. ≤60)	1,082	2.020 (1.465-2.784)	<0.001	2.101 (1.039-4.248)	0.039
Histological type (Infiltrating Lobular Carcinoma vs. Infiltrating Ductal Carcinoma)	977	0.827 (0.526-1.299)	0.410		
Race (White vs. Asian & Black or African American)	993	0.912 (0.615-1.350)	0.644		
radiation_therapy (Yes vs. No)	986	0.576 (0.394-0.841)	0.004	0.459 (0.248-0.850)	0.013
PCMT1 (High vs. Low)	1,082	1.512 (1.093-2.090)	0.012	2.088 (1.091-3.996)	0.026

BRCA: breast invasive carcinoma, ER: estrogen receptor.